REE geochemical exploration in magmatic felsic rocks and carbonatites of oceanic intraplate volcanic islands (the island of Fuerteventura)

Diego Greca Oteo

Academic advisors:

Dr. José Mangas Viñuela

M.Sc. Luis Ángel Quevedo González

Course 2019-2020

Final work to conclude Máster Interuniversitario en Oceanografía (ULPGC)

REE GEOCHEMICAL EXPLORATION IN MAGMATIC FELSIC ROCKS AND CARBONATITES OF OCEANIC INTRAPLATE VOLCANIC ISLANDS

(THE ISLAND OF FUERTEVENTURA)

Student: Diego Greca Oteo

Academic advisor: José Mangas Viñuela

Academic co-advisor: Luís Ángel Quevedo González

Vinculated investigation team: IOCAG (Instituto de Oceanografía y Cambio Global) and GEOGAR (Geología Aplicada y Regional).

_____   _____   _____

Dr. José Mangas Viñuela   M.Sc. Luis Ángel Quevedo González   Diego Greca Oteo

Facultad Ciencias del Mar   Facultad Ciencias del Mar   Facultad Ciencias del Mar

Instituto de Oceanografía y   Instituto de Oceanografía y   Master Interuniversitario en

Cambio Global, IOCAG   Cambio Global, IOCAG   Oceanografía

Universidad Las Palmas   Universidad Las Palmas   Universidad Las Palmas

de Gran Canaria   de Gran Canaria   de Gran Canaria

INDEX

ABSTRACT

Demand for Rare Earth Elements (REE) by industrialized countries in recent decades is high because due to the requirement to supply high-tech industries. Currently, China dominates the production and the REE market by 90% and that's why industrialized countries are focused on finding RE resources in their territories to avoid depending on the Chinese supply. REE deposits are mainly centered on complexes of alkaline magmatic rocks and carbonatites. For this reason, countries are carrying out geological exploration of these resources to try to alleviate the deficit of these critical elements for the industry. In this sense, the objective of the work has been focused on the geochemical exploration of REE in the complexes of alkaline igneous rocks and carbonatites from different periods, which emerge on the island of Fuerteventura. Thus, these rocks appear both in the Oligocene (34 to 23 Ma, group of submarine volcanic rocks, ultra-alkaline and plutonic complex of the basal complex), in the Miocene (23 to 12 Ma, shield volcanic complex) and in the Plioquaternary (<5.3 Ma, volcanic rejuvenation group). A total of 74 collected samples of alkaline igneous rocks and carbonatites from a 90s trip to Fuerteventura were geochemical analyzed. There were concentration data of 69 chemical elements for every sample: eight major (Si, O, Al, Mg, Fe, Ca, Na and K), four minor (Ti, P, Mn and H) and traces (eight REE included). Based on these data, binary and ternary geochemical diagrams for igneous rocks and carbonatites have been developed. Results confirm majority of igneous rocks are alkaline, subsaturated in silica, spatially and genetically related and are the result of a fractional crystallization process in the island's Oligocene magma chamber. Highest concentrations of REE are associated with carbonatites (ΣREE between 511 and 7372 ppm), felsic plutonic rocks (ΣREE between 51 and 2290 ppm) and, barely, with studied mafic and ultramafic rocks (ΣREE between 116 and 357 ppm). Furthermore, LREE concentrations are more important than HREE and Ce>La>Nd>Sm>Eu series is found. REE concentrations in felsic igneous rocks and carbonatites are very attractive, considering to develop mining plans. However, it would be necessary to select areas free of environmental and military limitations, and carry out detailed geological and geochemical exploration studies of REE plus economic valuation, to finally determine the future viability of mining.

1. Introduction

1.1. Rare Earth elements (REE)

In accordance with The Union of Pure and Applied Chemistry (IUPAC) the Rare Earth Elements (REE) include 15 lanthanides with the atomic numbers 57 to 71 in the periodic table: La, Ce, Pr, Nd, Pm, Sm, Eu, Gd, Tb, Dy, Ho, Er, Tm, Yb and Lu. It also includes Sc and Y (with atomic numbers 21 and 39 respectively) because both have physical and chemical properties that are very similar to the lanthanides. The term "rare" is used because REE are hard to find in considerable concentrations for economic extraction whose average concentration in the Earth's crust ranges from 150 to 220 mg kg^{-1}. In addition, this term is quite confusing because, for example, the most abundant REE, Ce, appears in Earth's crust in higher concentrations than Sn, Co and Mo; the rarest REE, Tm, is even more abundant than Au, Pt and Cd; Pm is an unstable element in nature and is part of uranium decay chain. According to the US Geological Survey, the 17 REE are divided into Light Rare Earth Elements (LREE) and Heavy Rare Earth Elements (HREE): LREE are comprised of elements with atomic numbers 57 through 63 (lanthanum to europium) while HREE have atomic numbers from 64 to 71 (gadolinium to lutetium). Scandium and yttrium are included within this last group because of the similar properties they share. On the other hand, LREE are more abundant usually than the HREE in the Earth's crust. Thus, all these elements have the same number of valence electrons in their last shell which is the structure $6s^2$. They are highly electropositive and reactive metals; their most common oxidation state is +3, although Ce, Pr and Tb can appear with +4 and Eu, Nd, Sm, Dy, Tm and Yb with +2; the bond is predominantly ionic and coordination number is usually bigger than VI. (Mancheri et al., 2013; Menéndez et al., 2019).

In recent decades, the study of mineral deposits of REE has advanced very rapidly. REEs represent about 0.02% by weight of the Earth's crust and rarely form their own minerals. However, REE-Y are forming part of more than 160 minerals in mineralogical classes such as oxides, silicates, phosphates, carbonates, halides, among others (Burt, 1989; Cesbron et al., 1989). Well-known deposits include some such as subsaturated alkaline igneous rocks, carbonatites, pegmatites, metamorphic rocks, paleosols or placers. World's most important deposits of subsaturated alkaline rocks are found in the alkaline massifs of Kibiny and Lovozero, both on the Kola Peninsula in Russia whose accessory mineral capable of hosting REE are perovskite, apatite and sphene. It is estimated that in Lovozero there are resources of more than 1000 Mt of ore with 0.8-1.5% REE_2O_3. In the case of carbonatites, which are igneous rocks constituted in more than 50% modal by primary magmatic carbonates, can generally accept a few hundred ppm REE (up to 6000 ppm), and they constitute a considerable reserve of other scarce elements such as Nb, Ta, Th, U, Zr, Ti, Cu, Zn, Mo, P, Ba, Sr and F, among others. For this reason, carbonatites are the mineral deposits with the greatest economic importance (Mariano, 1989 b) but they only represent 1% of the total volume of igneous rocks in Earth's crust. In addition, the interaction of hydrothermal fluids exsolved from the carbonatitic magma with hosts rocks produces REE enrichments in the phenytes generated. In addition, exogenous geological processes generate REE enrichments in supergene ore deposits. Several authors propose for the giant deposits of Bayan Obo (China) a model of hydrothermal formation, linked to carbonatites but developed in the carbonate host-rocks. Bayan Obo

is REE's largest known deposit so far, in terms of production (45% of world production) and reserves (135 Mt of ore with 6% of REE_2O_3).

In terms of applicability, rare earths are a critical component of several high technology goods (Morteani, 1991; Mancheri et al., 2013), such as hybrid vehicles, mobiles telephones, computers, televisions and, currently, are using in technologies within state-of-the-art green energies, such as efficiency enhancement of solar cells and artificial photosynthesis, based on H_2 generation. Current industry needs particular mixtures of RE and, therefore, interest is focused on reservoir that contain high purity REE, with particular interest in Sm, Nd and HREE. In addition, the prices of RE increase progressively, being heavy ones more expensive than light ones, depending on their cosmic abundance. Table 1 shows typical quantities of REE used in different products. (Mancheri et al., 2013; Menéndez et al., 2019).

Table 1. Quantities of REE used in different intermediate products. Modified from Mancheri et al., (2013).

Application	La	Ce	Pr	Nd	Sm	Eu	Gd	Tb	Dy	Y	Other
Magnets	-	-	23	69	-	-	2	0.2	5	-	-
Batteries	50	33	3	10	3	-	-	-	-	-	-
Metal alloys	26	52	6	17	-	-	-	-	-	-	-
Catalytic Converters	5	90	2	3	-	-	-	-	-	-	-
Catalysts	90	10	-	-	-	-	-	-	-	-	-
Polishing Compounds	32	65	4	-	-	-	-	-	-	-	-
Glass Additives	24	66	1	3	-	-	-	-	-	2	4
Phosphors	9	11	-	-	-	5	2	5	-	69	-
Ceramics	17	12	6	12	-	-	-	-	-	53	-
Other	19	39	4	15	2	-	1	-	-	19	-

In the world, China dominates the global Rare Earths Industrial Market as a result of a well-thought out carefully designed dynamic long-term strategy. Apart from raw materials, China controls also the production of key intermediates that are used in many growing high-tech industries. According to an US Government Accountability Office Report as of April 2010, China controlled: 97% of the REE ore; 97% of the RE oxides; 89% of the RE alloys; 75% of the Neodymium Iron Boron Magnets industry; 60% of the Samarium Cobalt Magnets industry. China's success in the world of RE is dependent of the continued use of RE intermediates in several key industries especially those facing a greener future (Mancheri et al., 2013). On the other hand, The European Commission estimates that the EU is 97% dependent on RE supplies from China. Europe is unable to meet today its industrial needs from the manufacturing sector due to high demand and limited availability of REEs being the Baltic Shield and South Greenland the main areas with a strong potential. Indeed, northern and southern Europe is characterized by several occurrences associated to alkaline magmatic complexes, carbonatites and placer deposits (Charles et al., 2013; Charalampides et al., 2015).

1.2. Geological setting

The Canary Islands, located between 27 and 30º north latitude, represent a hotspot track to find in the northwestern part of the African tectonic plate (Fig. 1). Thus, this archipelago, and more than twenty seamounts situated to the SW and N of Canary Islands, are of magmatic origin and they are related to an earth mantle anomaly (mantle plume), which gave rise to igneous activity for approximately 142 million years -Ma- (Fúster et al., 1968; Schmincke, 1976; Carracedo et al., 1998; Courtillot et al., 2003; Ancochea et al., 2004; van den Bogaard, 2013).

Fuerteventura is the easternmost island of this archipelago and together with Lanzarote represents the emergent crest of the Eastern Canarian Volcanic Ridge that lays out in a NE-SW trend, approximately parallel to the African continent margin, between 27.5° and 30.5° N latitude, and around 100 km offshore the Moroccan coast (Fig. 1). In addition, Fuerteventura is the oldest as well (34 and 23 Ma by its submarine and subaerial eruptions, respectively). This intraplate volcanic island is especial among oceanic islands due, firstly, to its location on a passive continental margin characterized by the absence of significant magmatism, secondly, to the unusually long time span of the magmatic activity because its activity started in the Oligocene, 34 Ma and continues until today), thirdly, to the surface presence of mesozoic oceanic lithosphere and oligocene submarine sedimentary and igneous rocks and, finally, to the existence of carbonatites outcrops.

In the island of Fuerteventura, three main geological units can be differentiated, from older to younger: the Basal Complex, the Miocene volcanic complexes, and the Pliocene-Quaternary sedimentary and volcanic rocks (Fig. 1). These units are described with detail below:

1) Basal Complex. This geological formation appear in the central western part of the island (Fúster et al., 1968; Robertson and Stillman, 1979; Le Bas et al., 1986; Fernández et al., 1997; Steiner et al., 1998; Balogh et al., 1999; Ancochea et al., 2004; Muñoz et al., 2005; Gutiérrez et al., 2006) and it is composed by (Fig. 1): i) the oceanic crust constituted by submarine volcanic (MORB, Mid-Ocean Ridge Basalt) and sedimentary rocks of Mesozoic age (early Jurassic and late Cretaceous) and ii) the Oligocene submarine and transitional volcanic groups with its associated plutonic bodies and dike swarms (Submarine and Emergent stages in the genetic model of oceanic intraplate volcanic islands of Walker, 1990). In relation to this second Oligocene ensemble (submarine volcanic in Fig. 1), deep submarine eruptions formed massive lava flows and pillowlavas on the Mesozoic oceanic crust, and later shallow eruptions gave place to pillowlavas, pillow breccias, hyaloclastites, lava deltas, debris flows and reef deposits; and subaerial volcanic group with basaltic and trachybasalts materials and debris flows. In relation to hypabyssal and plutonic rocks in this ensemble, an event of ultra-alkaline-carbonatitic plutonism took place at approximately 25 Ma (Ultra-Alcaline Complex in Fig. 1), comprising mainly different outcrops of ijolites, syenites and carbonatites in the central western part of the island (around Esquinzo-Agua Salada ravines in the La Oliva municipality, and coastal zones between Puerto de la Peña to Casas de Las Salinas in the municipalities Pájara and Betancuria). Besides, various alkaline ultramaphic, maphic and felsic plutonic rocks (wehrlites, pyroxenites, gabbros and syenites) intruded in the previous Oligocene host rocks, some of them formed ring complexes, producing

processes of contact metamorphism, partial fusion and metasomatism (Basal Complex Plutonics in Fig. 1). Finally, a swarm of dikes crosscut the set of units previously described in the basal complex. All these magmatic rocks are mostly Oligocene in age and they have been interpreted as submarine and transitional growth episodes of the Fuerteventura island.
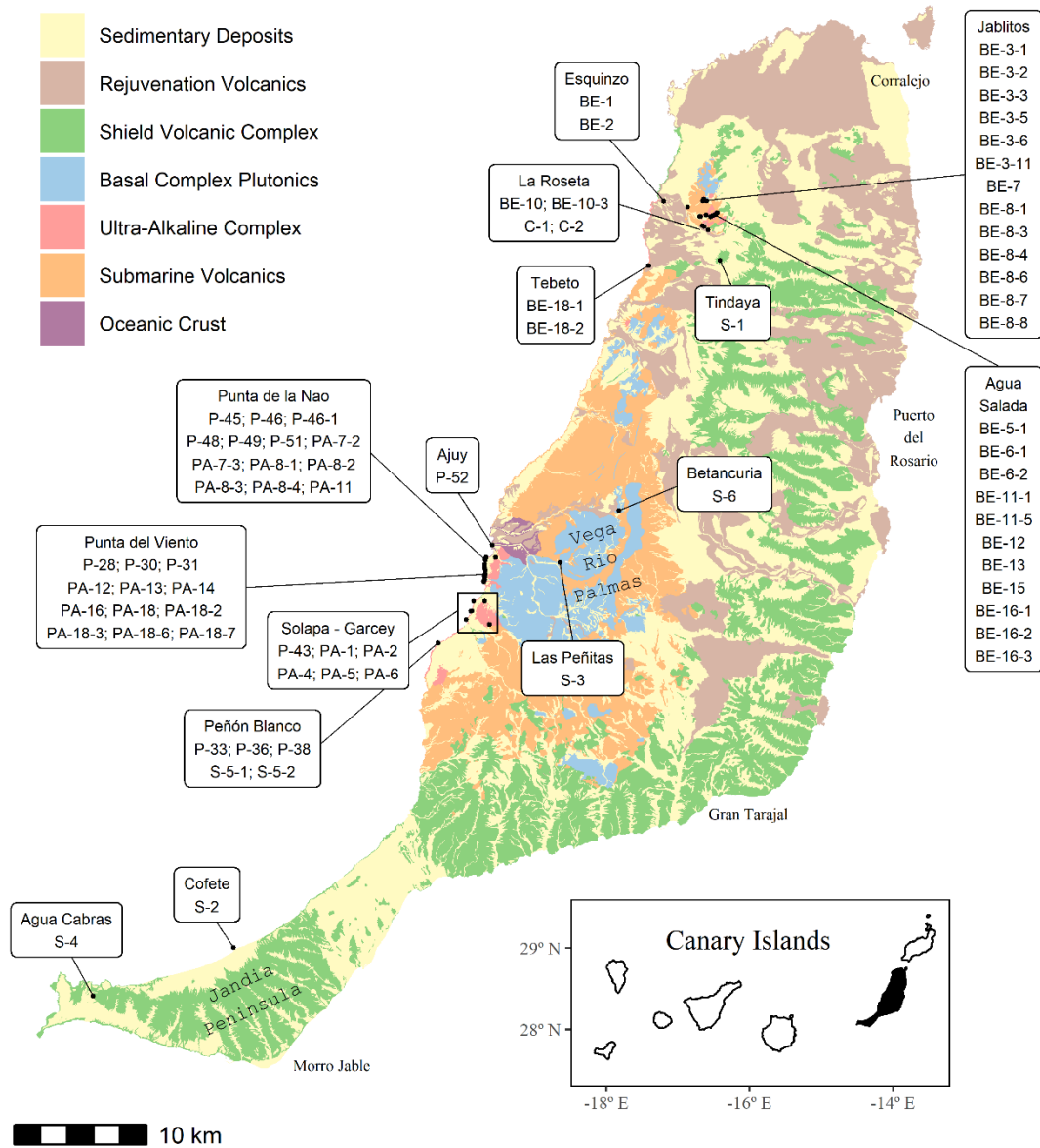
Figure 1. Location of the Fuerteventura island in the Canary Archipelago and simplified geological map of the island including main formations of every geological unit and the collected samples during this research.

2) Miocene Subaerial Volcanic Complexes. Three basaltic volcanic edifices were generated during the Miocene in Fuerteventura (Shield building and Declining stages of Walker genetic model, 1990, Shield Volcanic Complex in Fig. 1): the southern, central and northern volcanoes (Fúster et al., 1968; Coello et al., 1992; Balcells et al, 1994; Ancochea et al., 2004; Troll and Carracedo, 2016). The growth of each edifice was

marked by periods of volcanic inactivity associated with erosion and development of giant gravitational landslides. Thus, the central edifice, called Gran Tarajal, extends from Antigua town to the "El Jable" zone and it show three different constructive episodes between 22.5 and 14.5 Ma, containing basalt and trachybasalt materials (lava flows and priroclastic deposits). The northern edifice, as known as Tetir Edifice, includes two volcanic constructive episodes between 22 and 12.8 Ma, and they are constituted by basalts, picritic basalts, oceanitic basalts, trachybasalts and trachytes. The southern edifice emerges in the Jandía Peninsula and it was built by three successive constructive episodes between 20,7 to 14.2 Ma, and these made up of basaltic, ankaramite and trachybasaltic lava flows, hydromagmatic pyroclasts and quartz-trachytic plugs and tuffs.

3) Pliocene and Quaternary Sedimentary and Volcanic Rocks. A period of volcanic inactivity (erosive gap) followed the Miocene subaerial volcanic period and the edifices were deeply eroded, currently appearing as erosive remains in the landscape. Small basaltic strombolian volcanoes and associated lava fields later appeared from a renewed activity during the Pliocene (between 5.3 and 2.6 Ma) that has lasted until prehistoric times (Rejuvenation stage of Walker model, 1990; Rejuvenation Volcanics in Fig. 1). On the other hand, littoral and shallow water marine deposits and eolian, colluvial, alluvial and paleosol subaerial sedimentary formations were formed from the Pliocene to Quaternary along the entire surface of the island of Fuerteventura (Fúster et al., 1968; Zazo et al., 1997; Ancochea et al., 2004; Troll and Carracedo, 2016).

1.3. Geological characteristics of carbonatitic-alkaline felsic magmatic rocks in Fuerteventura

One of the world's REE exploration targets are the intrusive complexes containing alkaline felsic magmatic rocks and carbonatites. It turns out that these rocks appear in two of the main geological units are present on Fuerteventura: the Oligocene plutonic and subvolcanic rocks of Basal Complex (from 34 to 23 Ma) and the felsic intrusions related to the Miocene subaerially-erupted volcanic group (from 23 to 13 Ma).

Felsic hypabyssal-plutonic rocks (syenites, alkaline syenites, trachytes, quartz-trachytes, etc.) and carbonatites are associated to (Fig. 1): i) the Oligocene outcrops around Esquinzo-Agua Salada ravines, situated to the northwest of the island, and the Ajui-Casas de Las Salinas in the central-western coast, both containing ultra-alkaline ijolitic-syenitic complex with carbonatite bodies; and the syenites-gabbros ring dykes between Pájara and Betancuria towns; and b) Miocene felsic intrusives (stocks, plugs, dykes, etc.) related to the magmatic activity of the three stratovolcanoes (central, northern and southern), with outcrops all over the island (i.e. Tindaya mountain in the north or Cofete islet in the south).

The different felsic intrusives (domes, ring dykes, stocks, dykes, etc.) that occupy surfaces of several square kilometers and apophisis of decametric or metric dimensions. However, some ultra-alkaline carbonatitic outcrops show a structural and compositional extraordinary variability, appearing mixed pyroxenites, alkaline gabbros together with rocks of the ijolite-syenite series (melteigites, ijolites, nepheline syenites and syenites) and veins of calcium carbonatites (sovites and alvikites). In this sense, the alkaline-carbonatitic intrusive bodies appear as: a) dykes and veins metric and centimetric sizes distributed at random, with no defined directions and with no morphologic continuity due

to the fact that they are crossed by a thick mesh of later basaltic and, in minor amounts felsic, dykes which can occupy the 99% of the outcrop; b) show bad-defined contacts, with gradual and/or light diffused limits, sometimes assimilation structures between different bodies can be observed, and migmatite, mylonite and breccia structures due to presence of shear zones; c) textures from aphanitic to pegmatitic in the same body or adjacent bodies; d) sometimes they present metasomatism and fenitization processes, and partial melting and skarn zones due to contact metamorphism of subsequent intrusions, and e) these Oligocene magmatic outcrops are covered by Miocene and Plio-quaternary basaltic and sedimentary materials that makes it difficult to study them (Fúster et al., 1968; Barrera et al., 1981; Le Bas et al., 1986; Mangas et al., 1992; Fernández et al., 1997; Ancochea et al., 2004; Ahijado et al., 2005; Muñoz et al., 2005, Casillas et al., 2011).

The Oligocene and Miocene felsic outcrops are frequent in these complexes and appear as syenites, alkaline syenites, nephelinitic syenites, trachytes, quartz-trachytes, among others felsic igneous rocks. These materials are formed by K feldspar, aegirine and nepheline as primary minerals. However, its accessory and secondary minerals are very varied and have been cited in the bibliography, for instance, hornblende, biotite, apatite, zircon, andradite, vesubianite, plagioclase, sphene, Fe-Ti oxides, andradite, perovskite, zircon, monacite, sodalite, corindon, epidote, clinozoisite, albite, chlorite, sericite, quartz and calcite. In general terms, felsic plutonic rocks show values of percent by weight of % SiO_2 between 52 and >70%, and Na_2O+K_2O between 9 and 17%, and they are enriched in incompatibles elements, for example, Ba, Rb, Nb, Sr, Zr and REE, but they can have enrichment or depletion of some trace elements due to the processes of contact metamorphism, metasomatism and other geological alterations.

Carbonatites have been found on all the continents except Antarctica ranging in age from the Archean to the present distributed by different countries and these appear associated with hot spots, intracontinental rifts, transforming faults, subduction zones and continent-continent collision (Bell, 1989; Woolley, 1989), but they have only been identified at two oceanic locations (the Cape Verde and the Canary Islands). Carbonatites are composed by a big variety of mainly minerals: apart from carbonates (calcite, dolomite, ankerite or siderite), there may be variable proportions of spinel, ilmenite, bastnaesite, loparite, perovskite, apatite and various silicates and they are all enriched in REE, Y, Sr, F, S, among other trace element. Fuerteventura Oligocene carbonatites are composed essentially of calcite, and apatite, ore minerals, aegirine, K feldspar, diopside, sphene, biotite, hornblende, allanite, perovskite, pyrochlore, garnet, nepheline, cuspidine, baghdadite, and zircon appear as accessory minerals, and has been cited epidote, zoisite, sericite, chlorite, fluorite and albite as secondary minerals. Ore minerals are mainly magnetite and ilmenite, and in a lesser proportion pyrite, chalcopyrite, pyrrhotite, sphalerite, hematite, chalcocite, covellite and goethite. The REE in these carbonatitic bodies may be associated with the carbonates (bastnaesite), phosphates (britholite), silicates (allanite, sphene, zircon, epidote and stronalsite), and oxides and hydroxides (perovskite and goethite) (Barrera et al., 1981, Mangas et al., 1997; Fernández et al., 1997; Ahijado et al., 2005; Casillas et al., 2008; Casillas et al., 2011). These carbonatites have been generated as a magmatic differentiation product rich in CO_2 and they have been also deformed by shear zones and metamorphosed by late intrusive bodies.

1.4. Objective

The main objective representing this work is the REE geochemical exploration in magmatic felsic rocks and carbonatites of the island of Fuerteventura, mainly carbonatitic-alkaline plutonic Oligocene formation and, a lesser extent, felsic plutonic Miocene formation. Likewise, there is a series of specific objectives to be achieved during this study:

1) Geochemical classification of sampled volcanic and plutonic rocks using TAS diagrams (binary diagram of total silica-alkalis: SiO_2-Na_2O+K2O).
2) Analysis of major and minor element concentration (oxides) using Harker diagrams (binary diagrams of (wt. %) SiO_2 concentrations against (wt. %) MgO, FeO, CaO, Al_2O_3, Na_2O, K_2O, TiO_2, MnO_2 and P_2O_5 concentrations).
3) Search REE concentration anomalies with respect to the different study rocks.
4) Analysis of both compatible (Cr, Ni, Co, V, Sc, etc.) and incompatible (Rb, Ba, Sr, Nb, Zr, Y, etc.) trace elements (in ppm) as well as REE with the help of Spider and REE binary diagrams.
5) Exploitation feasibility of REE resources in Fuerteventura.

2. Methodology

2.1. Sampling

A total of 74 samples of magmatic-carbonate rocks were collected by geological research group GEOGAR (*Geología Aplicada y Regional*) belonging to IOCAG during a trip to Fuerteventura in 90 decades. Different geographic areas of the island were visited in order to subsequently obtain representative geochemical results (Fig. 2, Table 2): the largest of the rocks collected were plutonic rocks from the submerged edifice and the subaerial edifice (Oligocene and Miocene formations, respectively), as well as some volcanic rocks from other stages of the island growth.

2.2. Geochemical analysis

After collection, all the samples were prepared in the GEOGAR geological facilities and, then, they were sent to Activation Laboratories Ltd. (Actlabs, www.actlabs.com), specifically to the laboratory in Ancaster (Canada). This offers currently a formidable new analytical technology: the fourth generation inductively coupled plasma emission mass spectrometer (ICP-MS) combined with innovative lithium metaborate-tetraborate robotic fusion and inductively coupled plasma emission spectroscopy (ICP-OES). Fusion is performed by a robot at Actlabs, which provides a fast fusion of the highest quality in the industry. The geochemical analysis was made using the package Code 4E-research. This package uses ICP and INAA technologies to completely characterize geological samples with the concentration of 69 chemical elements between major and minor elements (% oxides) and trace elements (ppm or ppb):

- ICP: *Inductively Coupled Plasma*. For major elements, a 0.2 g sample was mixed with a mixture of lithium metaborate/lithium tetraborate and fused in a graphite crucible. The molten mixture was poured into a 5% nitric acid solution and shaken until dissolved. Samples were run for major oxides and selected traces on a Varian Vista ICP. For base

metals and selected trace elements, a 0.25 g sample was digested with four acids and heated using specific programmer which took every sample to dryness. After this, samples were brought back into solution using hydrochloric acid and finally, were analyzed using a Varian Vista ICP.

- INAA: *Instrumental Neutron Activation Analysis*. A 1 g aliquot was encapsulated in a polyethylene vial and irradiated along with flux wires at a thermal neutron flux. After a suitable decay, samples were measured for the emitted gamma ray fingerprint. INNA is very good for Au, Co, As, Sb, W, Ta, U, Th, Cs, In, Re, Cl and lower levels of most LREE.

Code 4E-research also included two options:

- Code 4E-XRF: elements Ga, Pb, Sn, Nb and Rb were examined by Pressed Pellet XRF. The trace elements analyses were done on pressed powder pellets from 6.5 g of sample. Spectral interferences were corrected from pre-calculated interfering factors. The detection limits are in general between 1 to 5 ppm.

Figure 2. Sampled outcrops during the field trip to Fuerteventura in 90 decades, containing different igneous rocks from submarine and subaerial geological formations.

Table 2. Geographic and geologic descriptions of 74 collected samples in the island of Fuerteventura.

Sample	Longitude	Latitude	Zone	Location	Magma	Product	Period	Lithological unit	
BE-1	595594	3167845	North	Esquinzo ravine, La Oliva	Silicate	Volcanic	Pliocene	Rejuvenation Volcanics	RV
BE-2	597395	3167415	North	Esquinzo ravine, La Oliva	Silicate	Volcanic	Oligocene	Submarine Volcanics	SV
BE-3-1	598545	3167876	North	Enamorados ravine, Jablitos, La Oliva	Silicate	Subvolcanic	Oligocene	Ultra-Alkaline Complex	UAC
BE-3-2	598545	3167876	North	Enamorados ravine, Jablitos, La Oliva	Silicate	Subvolcanic	Oligocene	Ultra-Alkaline Complex	UAC
BE-3-3	598545	3167876	North	Enamorados ravine, Jablitos, La Oliva	Silicate	Plutonic	Oligocene	Ultra-Alkaline Complex	UAC
BE-3-5	598545	3167876	North	Enamorados ravine, Jablitos, La Oliva	Silicate	Plutonic	Oligocene	Ultra-Alkaline Complex	UAC
BE-3-6	598545	3167876	North	Enamorados ravine, Jablitos, La Oliva	Silicate	Plutonic	Oligocene	Ultra-Alkaline Complex	UAC
BE-3-11	598576	3167866	North	Enamorados ravine, Jablitos, La Oliva	Mixed	Subvolcanic	Oligocene	Ultra-Alkaline Complex	UAC
BE-5-1	599614	3166988	North	Agua Salada ravine, La Oliva	Carbonate	Subvolcanic	Pliocene	Sedimentary Deposits	SD
BE-6-1	599583	3166923	North	Agua Salada ravine, La Oliva	Silicate	Plutonic	Oligocene	Ultra-Alkaline Complex	UAC
BE-6-2	599583	3166923	North	Agua Salada ravine, La Oliva	Silicate	Plutonic	Oligocene	Ultra-Alkaline Complex	UAC
BE-7	598845	3167859	North	Morro de los Jablitos, La Oliva	Silicate	Plutonic	Oligocene	Basal Complex Plutonics	BCP
BE-8-1	598608	3167982	North	Montañetas, Jablitos, La Oliva	Silicate	Plutonic	Oligocene	Ultra-Alkaline Complex	UAC
BE-8-3	598608	3167982	North	Montañetas, Jablitos, La Oliva	Silicate	Plutonic	Oligocene	Ultra-Alkaline Complex	UAC
BE-8-4	598608	3167982	North	Montañetas, Jablitos, La Oliva	Carbonate	Subvolcanic	Oligocene	Ultra-Alkaline Complex	UAC
BE-8-6	598608	3167982	North	Montañetas, Jablitos, La Oliva	Silicate	Plutonic	Oligocene	Ultra-Alkaline Complex	UAC
BE-8-7	598608	3167982	North	Montañetas, Jablitos, La Oliva	Silicate	Plutonic	Oligocene	Ultra-Alkaline Complex	UAC
BE-8-8	598608	3167982	North	Montañetas, Jablitos, La Oliva	Silicate	Subvolcanic	Oligocene	Ultra-Alkaline Complex	UAC
BE-10	598507	3165997	North	Esquinzo ravine, La Roseta, La Oliva	Silicate	Plutonic	Oligocene	Basal Complex Plutonics	BCP
BE-10-3	598643	3165921	North	Esquinzo ravine, La Roseta, La Oliva	Silicate	Subvolcanic	Oligocene	Ultra-Alkaline Complex	UAC
BE-11-1	598396	3166711	North	Agua Salada ravine, La Oliva	Silicate	Volcanic	Miocene	Submarine Volcanics	SV
BE-11-5	598301	3166700	North	Agua Salada ravine, La Oliva	Silicate	Volcanic	Miocene	Submarine Volcanics	SV
BE-12	599323	3166771	North	Agua Salada ravine, La Oliva	Silicate	Plutonic	Oligocene	Ultra-Alkaline Complex	UAC
BE-13	599140	3166670	North	Agua Salada ravine, La Oliva	Silicate	Plutonic	Oligocene	Ultra-Alkaline Complex	UAC
BE-15	598793	3166816	North	Agua Salada ravine, La Oliva	Silicate	Subvolcanic	Oligocene	Ultra-Alkaline Complex	UAC
BE-16-1	599532	3166868	North	Agua Salada ravine, La Oliva	Mixed	Subvolcanic	Oligocene	Ultra-Alkaline Complex	UAC
BE-16-2	599532	3166868	North	Agua Salada ravine, La Oliva	Silicate	Subvolcanic	Oligocene	Ultra-Alkaline Complex	UAC
BE-16-3	599532	3166868	North	Agua Salada ravine, La Oliva	Silicate	Subvolcanic	Oligocene	Ultra-Alkaline Complex	UAC
BE-18-1	594417	3162979	North	Tebeto beach, La Oliva	Silicate	Plutonic	Oligocene	Ultra-Alkaline Complex	UAC
BE-18-2	594488	3162981	North	Tebeto beach, La Oliva	Silicate	Plutonic	Oligocene	Ultra-Alkaline Complex	UAC
C-1	598945	3165661	North	Esquinzo ravine, La Roseta, La Oliva	Silicate	Volcanic	Pliocene	Rejuvenation Volcanics	RV
C-2	598945	3165661	North	Esquinzo ravine, La Roseta, La Oliva	Silicate	Volcanic	Pliocene	Rejuvenation Volcanics	RV
P-28	582087	3139473	Central	Caleta de la Cruz, Pájara	Carbonate	Subvolcanic	Oligocene	Ultra-Alkaline Complex	UAC
P-30	582106	3139650	Central	Punta de la Fuentecilla, Pájara	Silicate	Plutonic	Oligocene	Ultra-Alkaline Complex	UAC
P-31	582108	3139948	Central	Punta del Barquito, Pájara	Silicate	Plutonic	Oligocene	Ultra-Alkaline Complex	UAC
P-33	578531	3134448	Central	Punta Peñón Blanco, Pájara	Silicate	Plutonic	Oligocene	Ultra-Alkaline Complex	UAC
P-36	578563	3134419	Central	Punta Peñón Blanco, Pájara	Mixed	Subvolcanic	Oligocene	Ultra-Alkaline Complex	UAC
P-38	578565	3134420	Central	Punta Peñón Blanco, Pájara	Mixed	Subvolcanic	Oligocene	Ultra-Alkaline Complex	UAC
P-43	581077	3136867	Central	Punta de Don Blas, Pájara	Silicate	Plutonic	Oligocene	Ultra-Alkaline Complex	UAC
P-45	582112	3140705	Central	Punta de Caleta Mansa, Pájara	Silicate	Plutonic	Oligocene	Ultra-Alkaline Complex	UAC

P-46	582110	3140694	Central	Punta de Caleta Mansa, Pájara	Silicate	Plutonic	Oligocene	Ultra-Alkaline Complex	UAC
P-46-1	582108	3140702	Central	Punta de Caleta Mansa, Pájara	Carbonate	Subvolcanic	Oligocene	Ultra-Alkaline Complex	UAC
P-48	582150	3140848	Central	Punta de la Nao, Pájara	Silicate	Subvolcanic	Oligocene	Ultra-Alkaline Complex	UAC
P-49	582153	3140851	Central	Punta de la Nao, Pájara	Silicate	Subvolcanic	Oligocene	Ultra-Alkaline Complex	UAC
P-51	582860	3140904	Central	Aulagar ravine, Comisianes, Pájara	Silicate	Plutonic	Oligocene	Ultra-Alkaline Complex	UAC
P-52	582623	3141862	Central	Puerto de la Peña, Ajuy, Pájara	Silicate	Subvolcanic	Oligocene	Ultra-Alkaline Complex	UAC
PA-1	582407	3135845	Central	Majadas del Recogedero, Pájara	Silicate	Plutonic	Oligocene	Ultra-Alkaline Complex	UAC
PA-2	582073	3137594	Central	Solapa ravine, Pájara	Silicate	Subvolcanic	Oligocene	Ultra-Alkaline Complex	UAC
PA-4	581207	3137594	Central	Punta de la Canal, Pájara	Silicate	Plutonic	Oligocene	Ultra-Alkaline Complex	UAC
PA-5	580655	3136218	Central	Punta Jurada de Garcey, Pájara	Silicate	Plutonic	Oligocene	Ultra-Alkaline Complex	UAC
PA-6	581003	3136845	Central	Punta de Don Blas, Pájara	Carbonate	Subvolcanic	Pliocene	Sedimentary Deposits	SD
PA-7-2	582159	3140932	Central	Punta de la Nao, Pájara	Silicate	Plutonic	Oligocene	Ultra-Alkaline Complex	UAC
PA-7-3	582158	3140924	Central	Punta de la Nao, Pájara	Carbonate	Subvolcanic	Oligocene	Ultra-Alkaline Complex	UAC
PA-8-1	582135	3140792	Central	Punta de la Nao, Pájara	Carbonate	Subvolcanic	Oligocene	Ultra-Alkaline Complex	UAC
PA-8-2	582123	3140836	Central	Punta de la Nao, Pájara	Carbonate	Subvolcanic	Oligocene	Ultra-Alkaline Complex	UAC
PA-8-3	582135	3140826	Central	Punta de la Nao, Pájara	Carbonate	Subvolcanic	Oligocene	Ultra-Alkaline Complex	UAC
PA-8-4	582138	3140839	Central	Punta de la Nao, Pájara	Carbonate	Subvolcanic	Oligocene	Ultra-Alkaline Complex	UAC
PA-11	582091	3140759	Central	Punta de Caleta Mansa, Pájara	Silicate	Plutonic	Oligocene	Ultra-Alkaline Complex	UAC
PA-12	582068	3140360	Central	Laja de Gaspar González, Pájara	Carbonate	Subvolcanic	Oligocene	Ultra-Alkaline Complex	UAC
PA-13	582076	3140114	Central	Laja de Gaspar González, Pájara	Silicate	Plutonic	Oligocene	Ultra-Alkaline Complex	UAC
PA-14	582098	3139624	Central	Punta de la Fuentecilla, Pájara	Silicate	Subvolcanic	Oligocene	Ultra-Alkaline Complex	UAC
PA-16	582049	3139507	Central	Caleta de la Cruz, Pájara	Silicate	Plutonic	Oligocene	Ultra-Alkaline Complex	UAC
PA-18	582061	3139249	Central	Punta del Viento, Pájara	Silicate	Plutonic	Oligocene	Basal Complex Plutonics	BCP
PA-18-2	582053	3139242	Central	Punta del Viento, Pájara	Silicate	Plutonic	Oligocene	Basal Complex Plutonics	BCP
PA-18-3	581998	3139097	Central	Punta del Viento, Pájara	Silicate	Plutonic	Oligocene	Ultra-Alkaline Complex	UAC
PA-18-6	581987	3139089	Central	Punta del Viento, Pájara	Mixed	Subvolcanic	Oligocene	Ultra-Alkaline Complex	UAC
PA-18-7	582006	3139079	Central	Punta del Viento, Pájara	Silicate	Subvolcanic	Oligocene	Ultra-Alkaline Complex	UAC
S-1	599840	3163389	North	Tindaya dome, La Oliva	Silicate	Plutonic	Miocene	Shield Volcanic Complex	SVC
S-2	563078	3111398	South	Cofete Islet dome, Jandia, Pájara	Silicate	Plutonic	Miocene	Shield Volcanic Complex	SVC
S-3	587749	3140511	Central	Las Peñitas, Malpaso ravine, Betancuria	Silicate	Plutonic	Miocene	Basal Complex Plutonics	BCP
S-4	552460	3107740	South	Agua Cabras dome, Jandia, Pájara	Silicate	Plutonic	Miocene	Shield Volcanic Complex	SVC
S-5-1	578568	3134427	Central	Punta Peñón Blanco, Pájara	Silicate	Plutonic	Oligocene	Ultra-Alkaline Complex	UAC
S-5-2	578562	3134418	Central	Punta Peñón Blanco, Pájara	Carbonate	Subvolcanic	Oligocene	Ultra-Alkaline Complex	UAC
S-6	592203	3144453	Central	Las Peñitas ravine, Betancuria	Silicate	Plutonic	Miocene	Basal Complex Plutonics	BCP

\- Code 4E ICP-MS add-on option: can only be added to Code 4E research grade. Fused sample was diluted and analyzed by ICP-MS. Three blanks and five controls (three before sample group and two after) were analyzed per group of samples.

Code 4E-research detection limits (in ppm) of every analyzed element and the different laboratory techniques are shown in Annex Table 1 (oxides are represented in % while Au and Ir appear in ppb).

2.3. Data analysis

Firstly, to show correctly the situation of the samples and the characteristics of each area, the IDE Canarias (*Infraestructura de Datos Espaciales de Canarias*), the IGME (*Instituto Geológico y Minero de España)* and the IGNE (*Instituto Geográfico Nacional*) platforms were used. The first two provided geological data and the last one provided geographic information, all of them about Fuerteventura.

Then, Actlabs data analysis was done using first Microsoft Excel to perform recalculations on element concentrations in the samples to, sequentially, processed them using the R programming language version 3.6.3 (R Core Team, 2020) with additional packages: "ggplot2" version 3.3.2 for data visualization.

Finally, to interpretate results binary and ternary graphics were elaborated: TAS, R1-R2, Harker, Spider and normalized REE diagrams. These are frequently used in the treatment of geochemical data to classify igneous rocks and carbonatites, to find variations and geochemical trends, to see differences between abundance of major and minor elements and to analyze trace and REE in all the analyzed samples.

3. Results

In order to reach the objectives described widely in the section 1.4. the following results are exposed with detail and comprehensive explanations:

3.1. Geochemical classification of volcanic and plutonic rocks

Le Maitre (1984), with the help of experts from the IUGS commission, proposed the classification of volcanic rocks based on the chemical composition of SiO_2 and N_2O+K_2O presented by the geochemical analyzes of igneous rock samples (Fig. 3). It is a classification figure known as the TAS diagram (total alkali, silica, total Na_2O+K_2O and SiO_2), the main fields were delimited for volcanic rocks and, later for plutonic rocks (Wilson, 1989; Rollinson, 1993; Schmincke, 2004). Rocks are classified into four main groups: ultrabasic or ultramafic (<45% by weight of SiO_2), basic-mafic (45-52%), intermediate (52-63%) and acid (>63%). Intermediate and acidic rocks are also called felsic or salic rocks. Furthermore, the set of fields is divided into two large series of igneous rocks, which are alkaline (rich in alkalis) and subalkaline or tholeiitic (poor in alkalis) (Fig. 3). Within the alkaline ones, there are groups of rocks that reach the acid fields (rhyolites in volcanics and granites in plutonics) that are called alkaline supersaturated in silica, and those that don't reach this field are called undersaturated in silica.
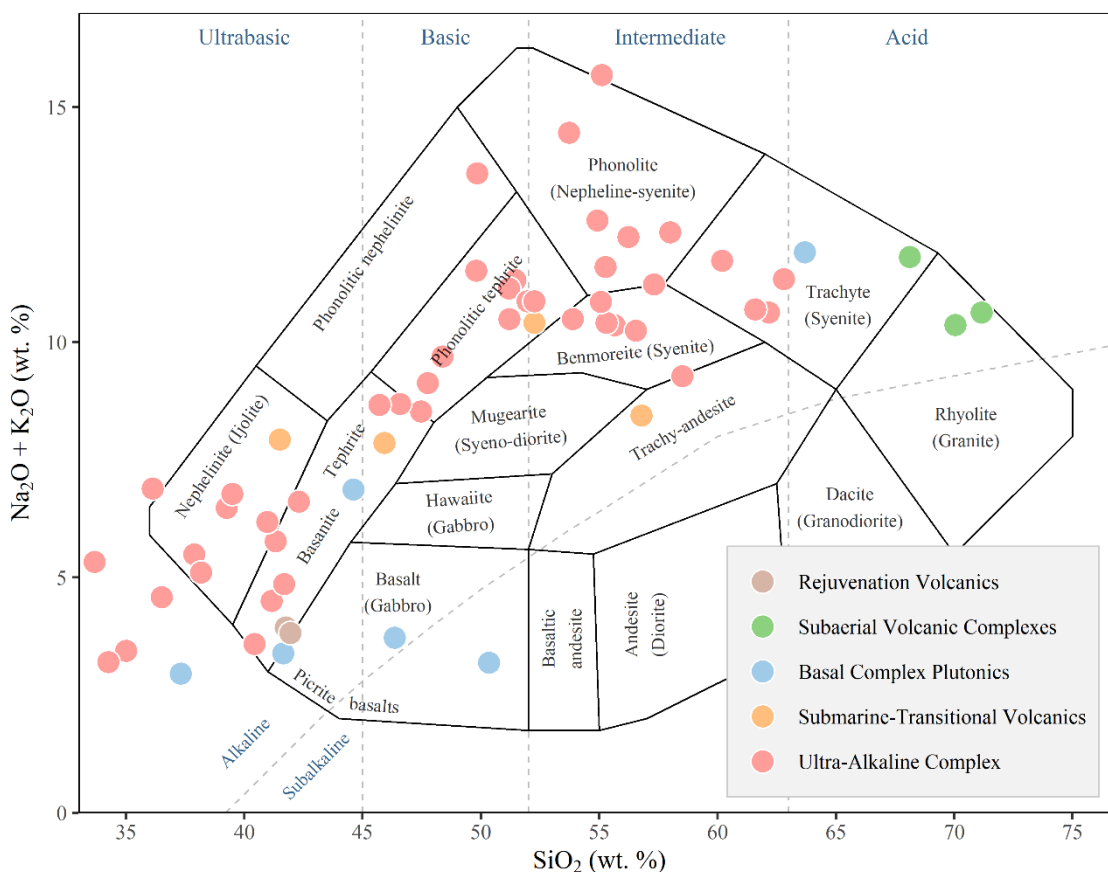

Figure 3. Diagram TAS which indicates the classification of studied volcanic and plutonic rocks based on the chemical composition of SiO_2 and Na_2O+K_2O (wt. %).

The geochemical results obtained in the Oligocene igneous rocks (Ultra-Alkaline Complex) and represented in Fig. 3, constitute an alkaline magmatic series subsaturated in silica, associated to a process of magmatic consolidation by fractional crystallization, so they have a clear genetic connection. Thus, it begins with the formation of ultrabasic rocks (ijolites, nephelinites and basanites), followed by basic rocks (in volcanic ones they would be basalts, tephrites, phonolitic tephrites and phonolitic nephelinites), then intermediate (syenites, nepheline syenites in plutonic and benmoreites and trachytes in volcanic) while rhyolitic or granitic rocks have not been sampled.

In our study, the geochemical data of the alkaline Oligocene plutonic rocks (Basal Complex plutonic) aren't very numerous and, thus, ultramafic rock samples are observed in the TAS (defined in the IGME geological cartography as peridotites of pyroxenites and werlites type), gabbros as plutonic and basanite as volcanic. On the other hand, there are mafic rocks analysis (gabbros as plutonic and basalts as volcanic); and intermediate sample of tephrite-phonolitic (dike in the Esquinzo ravine, which is from the northern Basal complex), and an acid sample from a syenite (La Peña ravine, near Ajuí). With this low number of samples, it's not possible to know if they form a complete alkaline magmatic series of fractional crystallization, although it's intuited in TAS, and there's only an intermediate composition. In turn, there are only three analyzed samples associated with Oligocene submarine volcanism and they show varied compositions: an ultramafic classified as nepheline and sampled in the Esquinzo ravine and a basic one (tephrite) collected in the Barranco de Agua Salada, both in the north. In addition, there's a sample of this group collected in the Barranco de Agua Salada that appears classified as tracy-andesite in the TAS diagram, but as it has a high percentage of volatile (LOI of 7%: CO_2 and H_2O), it could be altered with the consequent loss of alkalis and, therefore, could be classified as benmoreite. In relation to the Miocene plutonic rock analyzed samples, associated with felsic intrusives from subaerial Miocene edifices (outcropping domes in the south of Fuerteventura, Cofete islet and Cabras mountain, and Tindaya mountain in the north) and which have been classified in the TAS as syenite (dome of Cabras Mountain) and as alkaline granites (islet of Cofete and Tindaya mountain). These two acid rocks, as they are associated with subvolcanic or hypo-abyssal conditions, have been called quartz-trachytes in the geological cartography of Fuerteventura. Finally, from the Plioquaternary volcanic reactivation stage, two samples of lava were analyzed and they are ultramafic of basanitic composition from the Ventosilla edifice, and taken in the Esquinzo ravine.

If we use the classification diagram of plutonic rocks developed by De la Roche et al., (1980), which uses the parameters R1 (4Si – 11 (Na + K) – 2 (Fe + Ti) and R2 (6 Ca + 2 Mg + Al), calculated in millication proportions (Fig. 4), the ultramafic plutonic rocks of the Oligocene Ultra-alkaline complex fall in the fields of ijolites, melteijites, essexites and theralites, highlighting that some of these terms do not appear in the TAS classification of Le Maitre (1984), since there are empty fields without denomination in this graph of plutonic rocks used previously (Fig. 3). Also, mafic plutonic rock samples analyzed from the TAS diagram, fall on this R1/R2 diagram in the sieno-diorite fields. Regarding the intermediate and acidic rocks analyzed, they are classified as nepheline-syenite and syenite. Regarding the samples of the other plutonic groups, the Oligocene Ultramafic plutonic rocks of the Basal complex fall in the field of theralite and essexite, the basic ones like alkaline gabbro and gabbro, and the intermediate ones like syenite and

nepheline-syenite. In relation to the Miocene felsic intrusions associated with Shield volcanoes, they are syenite and quartz-syenite (this last petrological term is plutonic rock and the geological rock and cartography MAGNA calls it quartz-trachyte). The two Plioquaternary volcanic samples are basanites, theralites if they were plutonic. Finally, the three samples related to Submarine volcanism are essexite and ijolite for the ultramafic plutonics, and syenite for the intermediate rock.
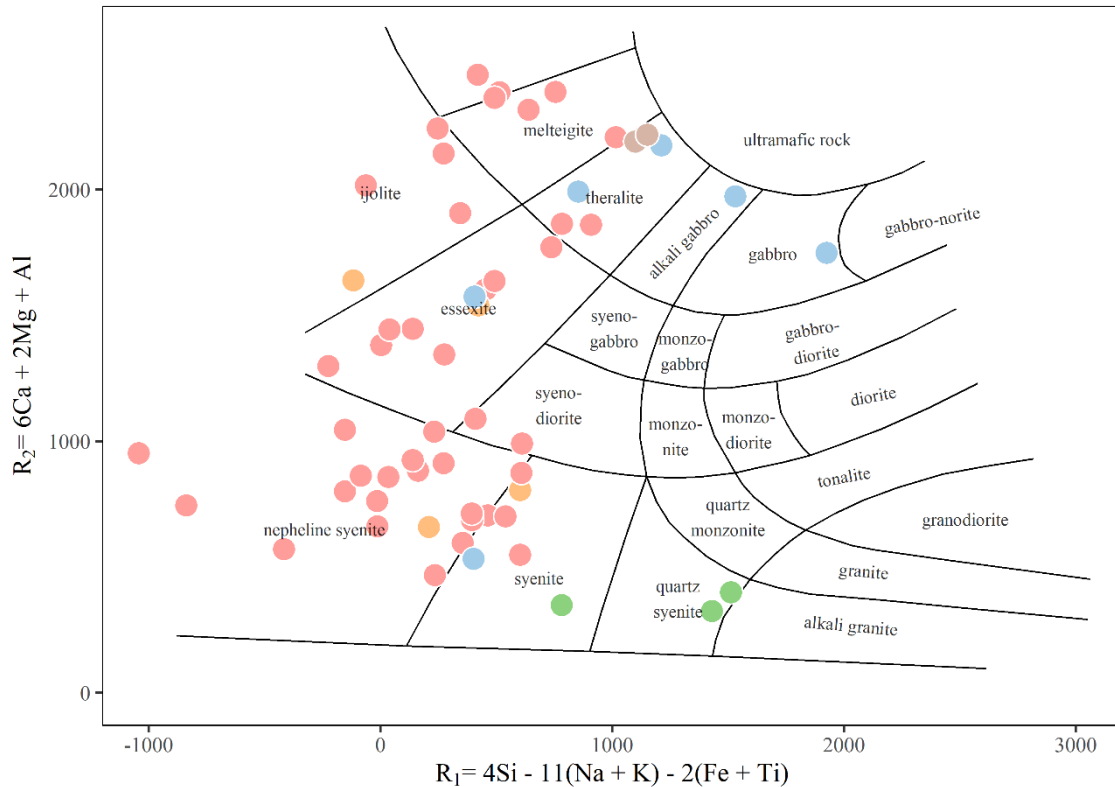
Fig. 4. Classification diagram of plutonic rocks developed by De la Roche et al., (1980) which uses parameters R1 and R2 in the studied samples of Fuerteventura island.

3.2. Analysis of major and minor oxides

Harker's chemical variation diagrams, wight percent of a constituent oxide is plotted against wt.% SiO_2 (binary plots, Fig. 5), show petrogenetic variations over time, such as fractional crystallization processes between the magmatic liquid and the formation of crystals in the chamber and characteristics of the mantle source (Wilson, 1989; Rollinson, 1993; Schmincke, 2004). The diagrams contain oxides of major elements, with concentrations in the Earth's crust above 1% such as Si, Fe, Mg, Al, Ca, Na and K and minor elements between 0,1 and 1% such as Mn, Ti and P. Variation diagrams are sometimes used in these petrogenetic studies with MgO values in wt.% or Zr values in ppm on the abscissa axis, compared to the oxides of the other major and minor elements on the ordinate (Wilson, 1989). Thus, for ensembles of genetically associated magmatic materials, pair of oxides are related either positively or negatively. Such correlation or trends can corroborate fractional crystallization processes, mixing of magmas by new injections in the chamber which is cooling, or contaminations of host-rocks. In this sense, trends on Harker diagrams are generally considered or represent the course of chemical evolution of magmatic chamber, during the natural cooling of magma over time with the

formation of major minerals (<95% of the total rock) or accessories (<5%). However, irregular or randomly distributed data, anomalous groupings of different data within these binary diagrams, can also indicate heterogeneities in the collected samples, such as very porphyry samples with megacrystals, which results in non-representative samples of outcrop, or analytical errors in the laboratory, both in the preparation of the samples and in their analysis.
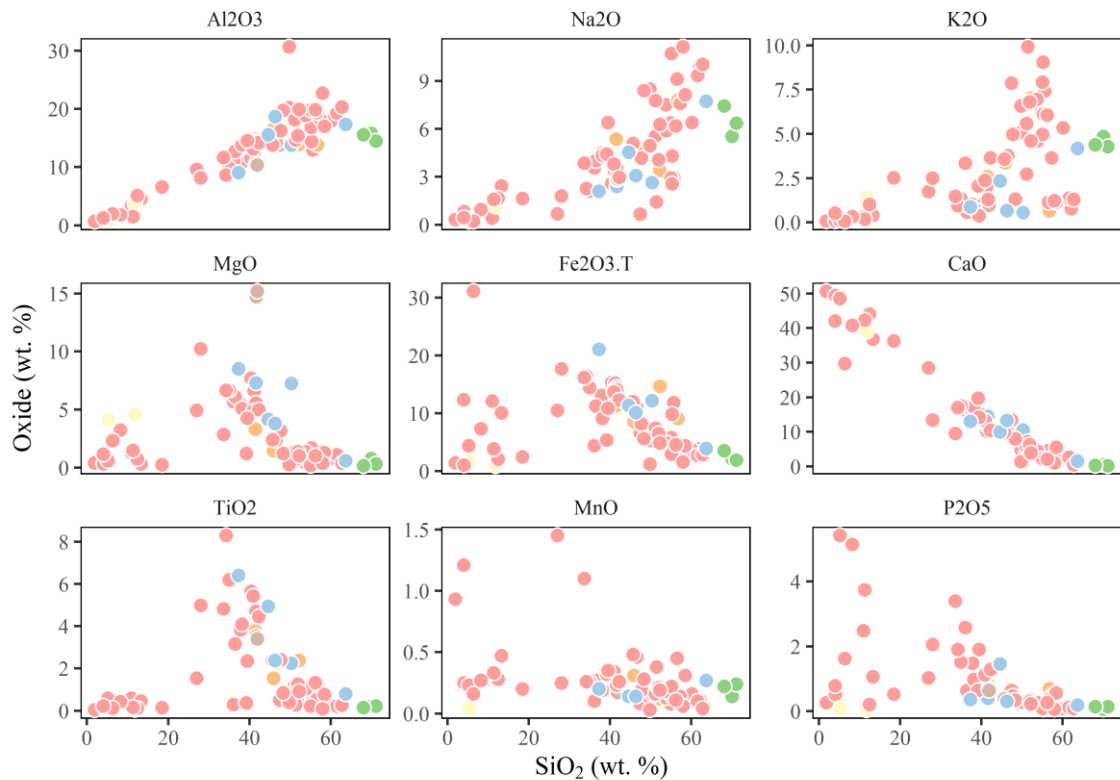
Figure 5. Harker's chemical variation diagrams: oxides of major and minor elements vs against wt.% SiO$_2$ in the studied samples in Fuerteventura.

Fig. 5 shows the Harker diagrams of the geochemical analyzes of our study, and it is observed that in the natural consolidation of magmas, going from ultramafic rocks to mafic to intermediate and acidic rocks, in other words, with the concentrations increase of wt. % SiO$_2$, there are clear increases in the concentrations of Al$_2$O$_3$, Na$_2$O and K$_2$O. This implies a positive trend among them. However, it shows a negative trend for oxides Fe$_2$O$_3$T, MgO, CaO, TiO$_2$ and P$_2$O$_5$. These trends of magmatic fractionation crystallization (magmatic differentiation) are very clear in rocks belonged to the Oligocene Ultra-alkaline complex, to a lesser extent in the plutonics of the Basal Oligocene complex since few rocks were sampled and in samples related to the Submarine volcanic Oligocene episode, the three Miocene Shield volcanoes and the Plioquaternary rocks of Volcanic rejuvenation. There aren't enough analyzes to see evolutions of these elements in their magmatic chambers. In the latter cases, the samples were taken to see the REE concentration of their most felsic terms and not to make a detailed study of their respective magmatic chambers. On the other hand, the high concentrations of Al$_2$O$_3$, Na$_2$O and K$_2$O in samples of Ultra-alkaline complex, indicates we are facing high Al rocks, ultra-sodium and ultra-potassium according to classifications doing by Wilson (1989) and Rollinson (1993). Similarly, observing Harker diagrams (Fig.

5), there are significant concentrations of CaO (mainly <20%), TiO_2 (<6%), Fe_2O_3 (<17%) and P_2O_5 (<2%) in ultramafic and mafic rock samples. However, they are moderate at low concentrations in MgO (<10%) and normal in Al_2O_3 (mainly <21%), MnO_2 (<0,5%), Na_2O (<9%) and K_2O (<7,5%), all of them within the series of alkaline igneous rocks.

On the other hand, the analyzed carbonatites have been classified and the geochemical obtained data are placed in a triangular CaO-MgO-$FeO + Fe_2O_3 + MnO_2$ diagram (Bell, 1989), the clear carbonatites of Fuerteventura are almost all calcium-carbonatites (fine-grained alwikites <1 mm and coarse-grained sovites >1 mm), as they have concentrations of CaO >80%, <18% of $FeO + Fe_2O_3 + MnO_2$ and <12% MgO (Fig. 6). On the other hand, brown-toned carbonatitic bodies containing dark ferromagnesian minerals and varied igneous rocks are classified as ferro-carbonatites, with CaO concentrations >35%, <55% of $FeO + Fe_2O_3 + MnO_2$ and <30% of MgO.

3.3. REE concentration and distribution

REE have similar chemical properties and their contents in rocks (igneous, metamorphic, and sedimentary) are frequently used for petrogenetic interpretations. Generally, REE plots have in abscissa the elements ordered by their atomic number, from smallest to largest, and in ordinate the quotient between the abundance values of the sample and a standard material. Thus, the REE plots compare REE abundances for different rocks graphically, normalizing the concentration of individual REE in a sample to their abundances in standard rocks (Wilson, 1989; Rollinson, 1993; Schmincke, 2004). Thereby, the concentration variation from element to element is observed, and differences or similarities are seen among them. For the study of REE in igneous rocks, different standard chondritic meteorites are used (Taylor and Mclennan, 1989; Rollinson, 1993), whose elements are considered as the concentration of the primitive earth mantle. From this primitive magma, a multitude of magmas have been formed over time, which have given rise to the igneous rocks that make up the igneous rocks of the earth's crust. In this sense, primitive mantle REE concentrations have been progressively depleted due abundant partial melting processes during the earth geologic history. LREE have a relative depletion in the earth mantle residuum, and since REEs are incompatible elements (they do not usually form their own minerals in fractional crystallization and accumulate in more evolved liquids forming some REE crystals), the ratios of LREE in a magma should essentially be similar to those in the mantellic source. Mantle minerals (olivine, pyroxene, garnet, spinel, mainly) do not concentrate LREE relative to the HREE. In general terms, the enrichment for a REE element to chondrite standard abundance depends on the initial concentration of that element in parental mantle, the degree of mantle partial melting and the subsequent crystallization in the magmatic chamber.
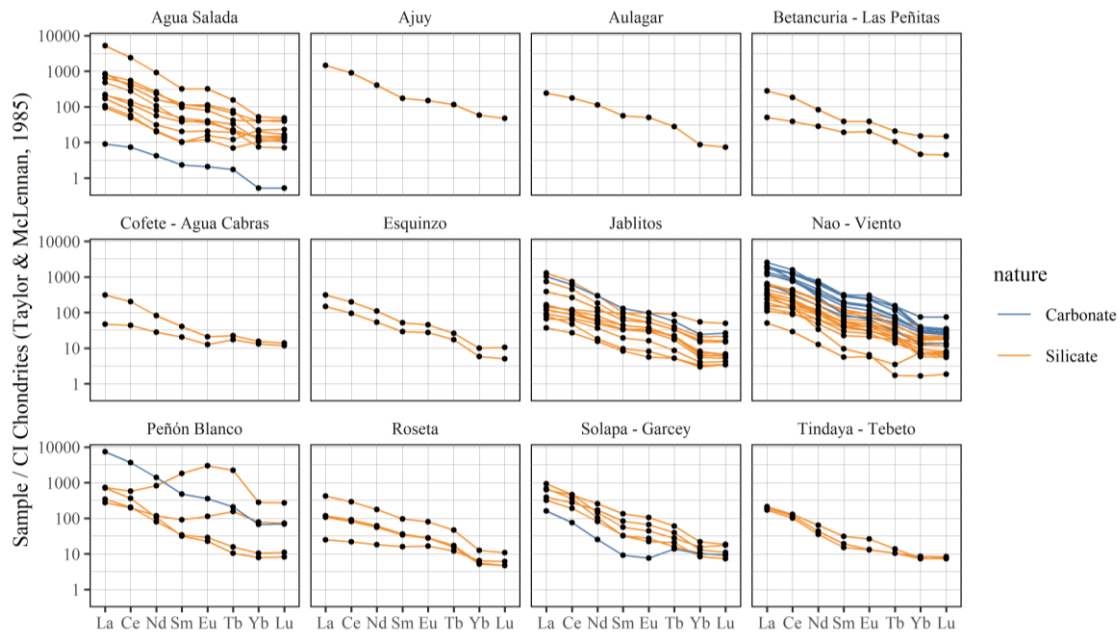
Figure 6. REE diagrams using chondrite-normalized REE of Taylor & McLennan, 1985 of studied samples in different geographic outcrops of Fuerteventura island, considering varied rock nature (carbonate/silicate).

REE plots of the samples analyzed in Fuerteventura are represented in Fig. 6 using as chondrite-normalized REE of Taylor & McLennan, 1985, and distributed by their geographical location, according to Fig. 1, and considering whether they are silicate or carbonate magmatic samples, including carbonatites and sedimentary carbonates. Thus, it is observed that if the values of the 74 samples were normalized, we would have straight lines parallel to unity (1) and therefore our rocks would have a composition and concentration of REE equal to the primitive mantle of the Earth, 4600 Ma ago. But as the mantle has undergone numerous partial melting and generated magmas during this time, the REE values of the magmatic rocks are those of the lower mantle below the Canaries area. In our case, the normalized values of LREE are higher than those of HREE in all samples, in such a way that the value of LREE / HREE is always greater than 1. In addition, they follow the same pattern, observing a descending line from the LREE to HREE, with some slight spike in Eu or Tb data. This Eu peak is frequent in Oligocene magmatic rocks (Agua Salada, Jablitos, Roseta in the north of the island; and Nao-Viento, Solapa-Garcey, Ajuí, Aulagar, Peñón Blanco in the center), Miocene (Betancuria- Las Peñitas), Plioquaternary (Tindaya-Tebeto in Jandía, in the south of the island). However, this peak in the value of Eu is not seen in Cofete-Agua Cabras in Jandía. Also, two silicate samples from the Punta de Peñón Blanco area (P-36 and P-38, which have high values of S and Ba, with the presence of the mineral barite), which follows an anomalous pattern in the form of bulging, and corresponds to silico-carbonatitic breccia associated with the ductile shear deformation zone. On the other hand, there are two carbonate samples (sedimentary, BE-5-1 in Agua Salada, and PA-6 in Solapa and Garcey) that show very low REE values in general and some below the standard chondrite. In turn, the normalized REE values are higher in carbonatite samples in relation to felsic silicate plutonic rocks (seen in Nao-Punta Viento, Jablitos, Punta Peñón Blanco). Also, the lines with the highest values in silicate rocks correspond to felsic rocks (intermediate and acidic) and the lowest

17

values to mafic-ultramafic ones, being observed well in the areas of Nao-Viento, Jablitos, Agua Salada, Roseta and Punta Peñón Blanco.

If we consider the ΣREE results from the geochemical analysis (Annex Table 2), the carbonatites present REE concentrations between 511 and 7372 ppm, and in the silicate magmatic rocks data between 51 and 2290 ppm for felsic rocks (intermediate and acidic) and for mafic and ultramafic rocks between 116 and 357 ppm. Therefore, there is a notable predominance of REE concentrations in carbonatitic rocks and, to a lesser extent, in felsic magmatic rocks.

3.4. Analysis of trace elements

The pattern of trace elements abundances in magmatic samples is useful to have a reference frame to which the elemental abundances in a particular rock can be compared (Wilson, 1989; Rollinson, 1993). The spider diagrams developing by Wood et al., 1979; Sun (1980); Thompson et al., 1984, among others, consider the abundances of a range of incompatible trace elements which are normalized to standard of a primary Earth mantle before crust formation (in our case the chondrite of Sun and McDonough, 1989, Fig. 8). The elements are arranged in decreasing incompatibility from left to right (Rb, Ba, Th…. Eu…. Y). The elements plotted all behave incompatible during the partial melting and fractional crystallization processes. There is an exception, the Sr, because it may be compatible with plagioclase (throughs in patterns), Ti with magnetite, and Y and Yb with garnet. These spider diagrams have peaks, throughs, slopes and curvatures of the patterns and they may provide petrogenetic information about crystallization processes. Spider diagram patterns are considered to be their mantle source and they are products of several partial melting processes. In general, the incompatible elements which are on the right-hand side should be enriched during partial melting, or for an alkalic oceanic-island basalt (OIB) extreme degrees of incompatible element enrichment with a peak at Nb-Ta are shown, suggesting that the source may also be enriched in incompatible elements. Sr, K, Rb and Ba are mobile in aqueous fluids and the rest are immobile.

The trace element concentration data of the studied samples are described in Annex Table 2. The abundance of compatible elements (Cr, Co, Ni, V, Sc, Co, etc.) appear, which become part of high-temperature ferromagnesian minerals by ionic substitution of Mg, Fe and Ca. The incompatibles (Cs, Pb, Rb, Ba, Th, U, Ta, Nb, K, P, Ti, REE, Y, among others), which are usually concentrated in liquids and waste fluids magma and do not usually form their own minerals, and there are ionic substitution of these elements by Ca, K, Na in felsic minerals. In our case, in the analyzed samples, high concentrations of trace elements stand out, with values above 500 ppm, such as, for example, Ba (<15000 ppm), Sr (<8000), Zr (<4000); Ce (<1500), Nb (<750), V (<650); between 100 and 500 ppm Cr (<300), Y (<300), Rb (<250), Ni (<200); and <100 ppm, the Co (<65) and Sc (<40). The most abundant in the treated samples are above all incompatible elements and these are the ones used in the spider diagrams.

Diego Greca Oteo

Figure 7. Chondrite-normalized diagrams (Spider diagrams) of incompatible elements (Sun & McDonough, 1989)

Spider diagrams produced (Fig. 7) have been arranged taking into account the samples collected in the outcrops of the different stages of formation on the island of Fuerteventura and separating the rocks of silicate composition (from ultramafic to acidic) and carbonate (carbonatites and caliches). Thus, the most modern are the Spider diagrams at the top (Plioquaternary volcanic sediments and Rejuvenation) to the oldest at the bottom (Ultra-alkaline complex and Oligocene submarine volcanism). In general lines, in the Oligocene samples of both the ultra-alkaline / carbonatite group of rocks and the basal complex plutonic, and the Miocene shield volcanic complex, very marked valleys of incompatible major and minor elements (K, P and Ti) are observed, along with Sr. On the contrary, peaks are seen in incompatible trace elements such as Ba, Nb, La, Zr, Nd, and occasionally in a few samples in Sm, U, Th. In the Plioquaternary sedimentary rocks only the valleys of K, P and Ti are observed. The carbonatites and silicate rocks of the Ultra-alkaline complex show lines with similar shapes, although higher values of incompatible elements such as LREE-Y and lower in K and Ti are observed in relation to the silicates. In addition, values of some incompatible elements are higher in this formation than in the others, being the least rejuvenating volcanic rocks.

4. Discussion

As indicated, the Canary Islands are associated with an oceanic intraplate hotspot that has been active for about 142 Ma (van den Bogaard, 2013). This hot spot is the manifestation in the oceanic crust of an anomaly of the lower terrestrial mantle in the archipelago area. Thus, the lower terrestrial mantle has suffered a slow ascent over millions of years, from about 2,900 to 660 km, according to tomographic results. Geochemical bibliographic studies of radiogenic isotopes in igneous rocks of the Canary Islands indicate that the lower mantle reservoir of magmas is heterogeneous, and is a mixture of the types HIMU + EM + DM (mixture of the subduced oceanic lithosphere component + mantle enriched in incompatible trace elements + mantle depleted in incompatible trace elements), according to Wilson, 1989; Ovchinnikova et al., 1995; Aparicio et al., 2003; Schmincke and Sumita, 2010; Troll and Carracedo, 2016, among other authors. Thus, the partial melting of this heterogeneous and anomalous mantle (around 10% fusion), generates alkaline ultramafic magmatic liquids in the upper mantle, more specifically in the area called asthenosphere, between 200 and 50 km, and these liquids rise and are they stagnate in magmatic chambers between 20 and 10 km deep (upper part of the upper mantle or base of the oceanic crust, called Mohorovicic seismic discontinuity).

These magmatic chambers with ultramafic liquids are active for hundreds of thousands of years or millions of years, and as time passes they lose temperature and different plutonic rocks are produced in depth and, if the pressures of the magma gases are sufficient, they are produced breaks in the oceanic crust, emitting magma on the surface and forming volcanic rocks in the island buildings (submarine eruptions first and subaerial later). The cooling process in the magmatic chambers forms different minerals that have different crystallization points from about 1800° C to hydrothermal conditions (<375ºC). These minerals form both plutonic rocks at depth and volcanic rocks at the surface, and the process of magmatic consolidation is called fractional crystallization or magmatic differentiation. Thus, we have ultramafic chambers with a lot of magmatic liquid and few crystals at high temperatures (<1400ºC), progressively generating ultramafic and mafic rocks, which are rich from the geochemical point of view in Fe-Mg-Ca-Ti and poor in Si-Al-Na-K, and containing fundamental minerals such as olivine, pyroxene, amphiboles, calcium plagioclase and Fe-Ti oxides. As the temperature in the chamber drops, the consolidation of the magma ends, with felsic rocks rich in Si-Al-Na-K and poor in Fe-Mg-Ca-Ti, called intermediate and acidic, and forming minerals such as alkaline feldspars, feldspathoids, plagioclase, biotite, sphene, apatite, quartz, among others, reaching temperatures of about 600ºC in the chambers, with a lot of solid, little liquid and many volatiles (CO_2, H_2O, F, S, P, etc.). These late felsic liquids and the volatile ones give rise to carbonatites made up of $CaCO_3$ and volatile minerals (sulfides, sulfates, fluorides, phosphates, etc.), in the case of Fuerteventura.

Taking into account this magmatic evolution, magmas generate ultramafic, mafic, intermediate and acidic rocks plus carbonatites, over time, and these fractional consolidation processes are reflected in the geochemistry of igneous rocks that appear in the geological history of each volcanic building on the islands or seamounts. However, it must also be considered that in addition to fractional crystallization, there may be magmatic reinjection processes in the chamber, giving rise to mixtures of magmas with different physical and chemical characteristics, contamination with cortical rocks,

increased or decreased melting rates partial, among others. Therefore, these different magmatic processes form igneous rocks with geochemical characteristics other than simple fractional crystallization.

In this work it has been geochemically verified (data and graphs TAS, R1 / R2, Harker, binaries of major oxides, of trace elements and REE figures normalized to chondrite) that the rocks of the ultra-potassium / carbonatitic and alkaline submarine plutonic formations of the basal complex, plus the acid rocks of the Miocene subaerial shield buildings (materials related to the alkaline decline stage of these edifices), are related to fractional crystallization processes of different magmatic chambers. This magmatic fractionation originates from ultramafic to acidic rocks (ijolite, melteigite, theralite, essexite, alkali gabbro, gabbro, nephelite syenite, syenite and quartz-syenite). The Oligocene silicate rocks analyzed are related to alkaline series subsaturated in silica, with ultra-alkaline samples (rich in K and Na) and peralumine (rich in Al), plus carbonatites, both in the outcrops of the north and center of Fuerteventura. However, the Miocene samples represent a silica-saturated alkaline series (quart-syenites and syenites) that appear in terms of the alkaline decline stage of stratovolcanoes in the felsic domes of Tindaya mountain in the north zone, and Agua Cabras mountain and Cofete islet.

Chemical elements in magmatic chambers form, in the early stages of fractional crystallization, fundamental ferromagnesian minerals (pyroxene such as augite-eyrine and diopside, amphiboles such as horblende and kaersutite, and oxides of Fe and Ti such as magnetite and ilmenite), feldspathoids (nepheline) and potassium feldspars (anorthoclase) in the ultramafic and mafic rocks, ending in the intermediate and acid rocks with more potassium feldspar, feldspathoid, biotite-phlogopite, plagioclase (albite) and quartz. The variety of accessory minerals (<5%) and secondary (alteration) is very high and they appear in a dispersed way in the outcrops, with numerous crystals of the groups of silicates, oxides, phosphates, sulfides, sulfates, fluorides, etc. (Fuster et al., 1968; Barrera et al., 1981; Mangas et al., 1994 and 1997, Muñoz et al., 2005; Casillas et al., 2008, Ahijado et al., 2005).

From the geochemical, petrological and mineralogical point of view, it is observed that in fractional crystallization there is an increase in Si-Al-Na and K and a decrease in Ca, Mg, Fe, Ti, P and Mn. In addition, their concentrations indicate that they are rocks richer in Ca, Ti, Fe, P and poor in Mg, than those studied in other oceanic islands intra-plate tholeiitic (Hawaii) and in the basalts of the oceanic bottom-MORB- in all oceans (Wilson 1989; Rollinson, 1993, Schmincke, 2004). The alkaline rocks subsaturated in silica and their minerals and geochemical graphs of Fuerteventura are more similar to those described for other archipelagoes such as, for example, in Tristan da Counha, Ascensión, Azores, Gough, Santa Helena in the Atlantic ocean, Tahiti, Marquesas and Society in the Pacific, and Kergulen in the Indian, but in each group of islands, island and stratovolcano there are peculiarities and differences in these geological factors. In addition, there are rare behaviors in some archipelagos, for instance, trends with tholeiitic and alkaline rocks in Reunión island or presence of tholeiitic and alkalic rocks contemporaneously in Galápagos islands. Thus, the variety of petrologic, mineralogic and geochemical data reflects different mantle source composition and partial melting degree, anomalies in fractional crystallization between alkalic and tholeiitic archipelago and in the oceanic ridges (Wilson, 1989; Rollinson, 1993, Schmincke, 2004; Schmincke and Sumita, 2010).

Diego Greca Oteo

Regarding the interpretation of the REE abundance values (Annex Table 2) and the trends in the graphs normalized to chondrite, we can affirm that the concentration and trend of this group of incompatible elements would be the same as that existed in the parent mantle that has partially melted in the area of the Canary Islands to give rise to this island. Thus, the mantle source and the subsaturated alkaline magmas of the Oligocene and Miocene formations are characterized by high concentrations of light REE and low in heavy ones. This behavior is typical of intraplate volcanic islands, where the partial melting of the mantle is low (around 10%) and a residue rich in garnet and possibly hornblende remains in depth (Wilson, 1989). Garnet and hornblende accumulate HREE and, by not melting, the concentrations of HREE and Y are low. However, by melting spinel, clinopyroxene, phlogopite and feldspar from the mantle source, they release the light rare earths, and therefore our rocks are richer in these elements. On the other hand, the LREEs released from the mantle accumulate in the last silicate fluids and melt in the consolidation of the magmatic chambers and, therefore, are more abundant in the more evolved rocks. These LREEs are in some of the minerals that make up primary carbonatites (Mangas et al., 1997), or those metamorphosed or tectonized by shear (mainly in britholite, monazite, allanite, pyrochlore, basnäesite, and, to a lesser extent, in barite, apatite and sphene). In lesser concentration, these LREE appear in felsic rocks (syenites, nepheline syenites and quartz-syenites) and in fundamentals such as potassium feldspars (anorthoclase), nepheline and plagioclase (albite), and also in accessories such as apatite or sphene. Feldspar precipitation can host cations such as Eu, but peaks of this element are only seen in late Oligocene plutonic rocks (Betancuria and Peñitas) and in Miocene rocks (Tindaya) (Fig. 6). Finally, the anomaly in the trends of the carbonate breccias of Punta Peñón Blanco, which is indicating that the fluids generated in the ductile shear deformation processes, there is the mobilization of REE and incompatible elements transported by aqueous-carbonic fluids rich in P, S and F. Therefore, anomalous REE trends are seen in this shear band, different from those observed in the other rocks analyzed and that do not correspond to a particular primary mantle.

Carbonatite bodies sampled in the different outcrops are highly variable, since there are dikes and bodies of homogeneous light tones essentially made up of calcium carbonate (calcite). Other outcrops are spangles of a few decimeters or square meters since they are crossed by posterior intrusions (mainly basaltic dikes) of light and dark tones since they have undergone contact metamorphism and metasomatism with new mineral recrystallization (neoformation). Finally, those that are located in shear bands of darker tones, less than 25 m wide, and crossed by dikes as well, and where carbonatites appear brecciated and mylonitized by the deformation of ductile shears, together with mafic and felsic rocks, more basaltic dikes. The light carbonatites predominate the calcite, but in the light-dark and dark ones, in addition to calcite, there are silicates, oxides, phosphates, sulfides, among other groups of minerals, together with fragments of igneous rocks of different geochemical composition. This variety of outcrops means that the clear carbonatites of Fuerteventura are almost all calcium-carbonatites (fine-grained alwikites <1 mm and coarse-grained sovites >1 mm) and brown-toned carbonatitic bodies containing dark ferromagnesian minerals and varied igneous rocks

Regarding the interpretation of the results of the incompatible trace elements normalized with the chondrite pattern, and exposed in the Spider diagrams (Fig. 7), we can confirm that these traces characterize the primary mantle source and the parent magmas from

which they come the rocks. Thus, for the magmas of the Canary Islands we observe that the normalized values of K, P, Ti and Sr are low and they develop valleys in the graphs, especially in the carbonatites. Therefore, they announce that these elements have already been fixed in minerals of felsic rocks (K and Sr in feldspars, Sr in epidote, apatite and stronalsite, P in apatite or britholite, and Ti in oxides of Fe and sphene), so the carbonate fluids are more depleted in them. These low values in K, P and Ti have already been cited by other authors for rocks from different Canary Islands (Ancochea et al., 2004), and for other archipelagos such as Madeira, Santa Helena, Marquesas, etc. (Wilson, 1989), so the mantle source and the magmatic liquids generated are poor in these elements. On the other hand, a series of peaks or positive anomalies are defined in Fig. 8, in elements such as Ba, Nb, La, Zr and Nd (and specifically Sm, U, Th in very rare samples), indicating that the parent fluids are rich in these elements. These enrichments give rise to minerals containing them. For example, Ba is associated with sulfate in the form of Barite; Nb to pyrochlore; the La, Nd and other REE-Y to britholite and basnäesite-synchisite, apatite and sphene; and Zr in sphene or zircon or minerals of the niocalite-cuspidine series, accessory or accidental minerals present in rocks evolved from complexes (intermediate and acidic) and in carbonatites (Mangas et al., 1997). The presence of U and Th in some samples is due to the presence of the mineral zircon (SiO_4Zr), since ionic substitutions of zirconium by these elements occur. On the other hand, Ba (or Rb) can substitute for K in potassium feldspars (anorthoclase), hornblende and biotite, which are frequent minerals in felsic rocks and carbonatites.

In Fuerteventura, the REE concentrations determined in this work in alkaline igneous rocks and carbonatites are interesting (grades lower than 7372 ppm in carbonatites and <2290 in felsic rocks). However, LREEs (Ce, La, Nd, Sm and Eu) predominate in the rocks, and HREE have low concentrations, so the resources would have a lower economic value, at the current price of the mineral market. It has been corroborated that from the point of view of mining exploration the carbonatites of the ductile shear zones of Punta del Peñón Blanco and Caleta de la Cruz stand out, and the bodies of carbonatites and intrusive igneous felsic rocks of the Aulagar ravine and Punta de Nao- Solapa, in the center-west of the island, along with veins, breccias and sejones of carbonatites and felsic rocks in the area of the Esquinzo ravine, Agua Salada and Jablitos, in the island north. Therefore, the data from the alkaline igneous and carbonatite rocks of Fuerteventura have a certain economic potential to take into account. On the other hand, outcrops with mining interest have a series of environmental and military limitations since. i) The areas with interesting content in REE are located in protected coastal strips within the Terrestrial Maritime Public Domain (DPMT) and the Protective Easement Zone (100 meters inland, expandable up to 200 meters), according to the Coastal Law 2 / 2013; ii) some outcrops with metallogenic interest are within areas protected by Canarian law (Law 12/1994, for example, in the north, the Tindaya Mountain Natural Monument, in the Betancuria Rural Park and the Ajuí Natural Monument, in the south Jandía Natural Park), or by European legislation of Red Natura 200 with the cataloging of ZEC (areas of special conservation such as, for example, in the center Betancuria 13_FV and Cueva de Lobos 22_FV, and in the south Jandía 17_FV; (bird protection area) such as, for example, Lajares, Esquinzo and Costa de Janubio (101), Betancuria (97), or Jandía (39); iii) some outcrops of the central zone are within the military shooting range of Pájara that goes from the Barranco de la Solapa to the south. Consequently, areas with environmental or military protection,

both REE's detailed exploration and exploitation, if feasible, would be unviable for these reasons. In addition to this, there are the Island Management Plans (PIO) and the PORN natural resource management plans for the protected areas of Fuerteventura, which should be reviewed and future mining extraction proposals approved. In both cases, the review and approval of the plans, defining the extractive uses of raw materials, could take years. Consequently, the viability of exploitation of RE resources associated with the geological outcrops of carbonatites and felsic igneous rocks that appear on the surface in Fuerteventura is low, according to the data available to date. New detailed mining exploration work would have to be carried out (pits and exploration wells with sample collection, analysis, valuation, cubing and economic evaluation) in the areas where this type of rocks outcrop and that have no restricted uses, due to environmental limitations, military or land uses. In this way, it would be possible to know exactly the possibilities that surface carbonatites and felsic magmatic rocks have, plus those that are covered by later rocks, both of igneous and sedimentary origin.

5. Conclusions

The main objective of this work was the REE geochemical exploration in magmatic felsic rocks and carbonatites of the island of Fuerteventura, mainly in the Oligocene plutonic carbonatitic-alkaline formation and, to a lesser extent, in the Miocene plutonic felsic formation. These rocks belong to the Oligocene phase of submarine construction of the island and to the stage of decline of the Miocene volcanic edifices. The treatment and interpretation of the data on the concentration of major, minor and trace elements from the total rock chemical analysis of more than 70 samples, preparing calculations and graphs commonly used in geochemical studies, has allowed conclusions to be drawn to the different partial objectives set in this study, and are detailed below:

(i) Geochemical classification of sampled igneous rocks, using binary diagrams (TAS total silica-alkalis of Le Maitre, and R1-R2 of De la Roche), confirms the oligocene ultra-alkaline plutonic complex is formed by ultramafic (ijolites, melteigites, theralite and essexite), mafic (syeno-diorite), and intermediate-acid (nepheline-syenite and syenite) rocks, within the subsaturated sub-alkaline magmatic series. Carbonatites are calcium-carbonatites and ferro-carbonatites and last to form. These magmatic rocks have been generated in a fractional crystallization process and are spatially and genetically related, although some of them have undergone subsequent processes of contact and regional metamorphism, metasomatism, and ductile shear deformations. The plutonic formation of the basal complex, intruded later but also of Oligocene age, is intuited in the analysis that it comes from another fractional crystallization process and another magmatic chamber, with terms ranging from ultrabasic to acidic (theralite, essexite, alkali gabbro, gabbro, nephelite syenite and syenite). Miocene felsic rocks come from a different magma chamber and only the most evolved rocks that are acidic and classified as syenite and quartz syenites have been analyzed.

(ii) Analysis of major and minor element concentration (oxides) using Harker diagrams and oxide against oxide corroborate that fractional crystallization in magmatic chambers there is an increase in silica as the temperature decreases until its consolidation together with $Na_2O + K2O$ and Al_2O_3, while there is a decrease in the oxides of Ca, Fe, Mg, Ti, P and Mn. Some of the plutonic rocks analyzed, in addition to being ultra-alkaline (ultra-potassium and ultrasodic) and peralkaline (high Al_2O_3).

(iii) Search REE concentration anomalies with respect to the different study rocks has confirmed that the carbonatite bodies have the highest concentrations (<7372 ppm), followed by felsic plutonic rocks (intermediate and acidic, <2290 ppm) and the lowest mafic and ultramafic values (<357 ppm). There is a predominance of LREE over HREE (LREE / HREE >1), and it is true that the concentration of Ce> La> Nd> Sm> Eu. Therefore, the mantle source and the subsaturated alkaline magmas generated, from the Oligocene formations of the submarine edifice to the subaerial Miocene, are characterized by having high concentrations of light REE and low in heavy REE and Y, so we have a low partial fusion rate of the primitive mantle (about 10%) under the Canaries and there is a mantle residue rich in garnet and hornblende, which contains the HREE. Furthermore, the liquids are enriched in LREE, with significant peaks in Eu and Yb in relation to the chondritic pattern used. Furthermore, in the REE diagrams normalized to chondrite, trends with high values of carbonatites are observed, followed by felsic plutonic rocks and the minimum values occur in mafic and ultramafic rocks.

(iv) In relation to the abundance of compatible and incompatible trace elements in the analysis carried out, concentrations >500 ppm in Ba (<15000 ppm), Sr (<8000), Zr (<4000) stand out; Ce (<1500), Nb (<750), V (<650); between 100 and 500 ppm Cr (<300), Y (<300), Rb (<250), Ni (<200); and under 100 ppm are Co (<65) and Sc (<40). Considering the incompatible elements treated in the spider diagrams, negative anomalies of K, P and Ti and Sr, and positive anomalies are observed in Ba, Nb, La, Zr, Nd, both in the ultra-alkaline/carbonatitic Oligocene rocks and the basal plutonic complex ones as in the volcanic complex of the Miocene shield. Therefore, the primitive mantle and parent magmas exhibit these particular geochemical characteristics. However, in the spider diagrams can be seen differences in each geological stage of the Fuerteventura formation, so there are different alkaline magmas with differences in the values and trends of incompatible trace elements in the submarine and subaerial construction of the island.

(v) REE resources in the outcrops of the ultra-alkaline/carbonatitic and alkaline Oligocene plutonic formations, and the felsic Miocene plutonic in Fuerteventura, are significant due to their moderate to high grades, and a future mining project could be planned. However, it must be taken into consideration that some outcrops of these igneous rocks have geological limitations (they are irregular, discontinuous and not very extensive), environmental (within protected areas and coastal areas) and military (Pájara shooting range). Therefore, it would be necessary to select outcrops of these alkaline felsic magmatic rocks and carbonatites that don't have these limitations, and plan a detailed geological, geochemical and mining exploration, carrying out geological cartography, a detailed sampling mesh, and in each sample make petrographic, mineralogical and geochemical analysis. With these data and by analyzing information on extraction costs, mineral treatment and market prices of these raw materials, its economic viability of exploitation in the medium term could be determined.

6. Bibliography

Actlabs. 2020. Activation Laboratories Ltd. (Actlabs) - Analytical Lab Services. Available at: <https://actlabs.com/>

Ahijado, A.; Casillas, R.; Nagy, G. & Fernández, C. (2005). Sr-rich minerals in a carbonatite skarn, Fuerteventura, Canary Islands (Spain). Mineralogy and Petrolology, 84 (1-2): 107-127.

Ancochea, E. & Barrera, J.L. & Bellido, F. (2004). Canarias y el vulcanismo neógeno peninsular. Geología de España. 635-682. Aparicio, A., Hernán, F., Cubas, C.R. y Araña, V. (2003). Fuentes mantélicas y evolución del volcanismo canario. Estudios Geológicos, 59, 5-13.

Balcells, R.; Barrera, J.L.; Gómez, J.A.; Cueto, L.A.; Ancochea, E.; Huertas, M. J.; Ibarrola, E. & Snelling, N. (1994). Edades radiométricas en la Serie Miocena de Fuerteventura. (Islas Canarias). Bol. Geol. Min., 35: 450-470.

Balogh, K.; Ahijado, A.; Casillas, R. & Fernández, C. (1999). Contributions to the chronology of the Basal Complex of Fuerteventura, Canary Islands. Journal of Volcanology and Geothermal Research, 90: 81-102.

Bell, K. (1989): Carbonatites: genesis and evolution. Ed. Unwin Hyman. London, 601 pp.

Burt, D.M. (1989). Compositional and pase relations among rare earth element minerals. In: Geochemistry and mineralogy of rare Earth elements. Rev. In Mineralogy. Publ. The Mineralogical Society of America, 21, 259-308.

Carracedo, J.C., Day, S., Guillou, H., Rodríguez, E., Canas, J.A., Pérez, F.J., 1998. Hotspot volcanism close to a passive continental margin. Geol. Mag. 135, 591-604.

Casillas, R.; Démeny, A., Nagy, G.; Ahijado, A. & Fernández, C. (2011). Metacarbonatites in the Basal Complex of Fuerteventura (Canary Islands). The role of fluid/rock interactions during contact metamorphism and anatexis. Lithos, 125, 1-2: 503-520.

Casillas, R.; Nagy, G.; Demény, A.; Ahijado, A. & Fernández, C. (2008). Cuspidine–niocalite–baghdadite solid solutions in the metacarbonatites of the Basal Complex of Fuerteventura (Canary Islands). Lithos 105: 25-41.

Cesbron F. P. (1989). Mineralogy of the rare-earth elements. In: P. Möller, P. Cerny and F. Saupé (eds), Lanthanides, tantalum and niobium, Sp. Pub. Nº 7 SGA. Springuer Verlag,3-27.

Charalampides, Georgios & Vatalis, Konstantinos & Baklavaridis, Apostolos & Benetis, Nikolas-Plutarch. (2015). Rare Earth Elements: Industrial Applications and Economic Dependency of Europe. Procedia Economics and Finance. 24. 10.1016/S2212-5671(15)00630-9.

Charles, N., Tuduri, J., Guyonnet, D., Melleton, J., & Pourret, O. (2013). Rare earth elements in Europe and Greenland: a geological potential? An overview. *12th Biennial SGA Meeting*, (August), 12–15.

Coello, J.; Cantagrel, J.M.; Hernán, F.; Fúster, J.M.; Ibarrola, E.; Ancochea, E.; Casquet, C.; Jamond, C.; Díaz de Teran, J. R. & Cendrero, A. (1992). Evolution of the Eastern Volcanic Rigde of the Canary Islands Based on New K-Ar Data. Journal of Volcanology and Geothermal Research, 53: 251-274.

Courtillot, V., A. Davaille, J. Besse & J. Stock (2003). Three distinct types of hotspots in the Earth's mantle. Earth and Plan. Sc. Let. 205: 295-308.

De la Roche, H., Leterrier, J., Grandclaude, P., & Marchal, M. (1980). A classification of volcanic and plutonic rocks using R1R2-diagram and major-element analyses — Its relationships with current nomenclature. *Chemical Geology*, *29*(1), 183–210.

Fernández, C.; Casillas, R.; Ahijado, A.; Perelló, V. & Hernández-Pacheco, A. (1997). Shear zones as a result of intraplate tectonics in oceanic crust: the example of the Basal Complex of Fuerteventura (Canary Islands). Jour. Struct. Geol, 19, 1: 41-57.

Fúster, J.M.; Cendrero, A.; Gastesi, P.; Ibarrola, E. & Lopez Ruiz, J. (1968). Geología y volcanología de las Islas Canarias- Fuerteventura. Instituto "Lucas Mallada". Consejo Superior de Investigaciones Científicas, Madrid. 239 pp.

Gutiérrez, M.; Casillas, R.; Fernández, C.; Balogh, K.; Ahijado, A.; Castillo, C.; Colmenero, J.R. & García-Navarro, E. (2006). The submarine volcanic succession of the Basal Complex of Fuerteventura, Canary Islands: a model of submarine growth and emersion of some tectonic-volcanic Islands. Geological Society of American Bulletin, 118 (7/8): 785-804.

Le Bas, M.J.; Rex, D.C. & Stillman, C.J. (1986). The early magmatic chronology of Fuerteventura. Geol. Mag., 123: 287- 298.

Le Maitre, R.W. (1984). A proposal by the IUGS subcomission of the systematics of igneous rocks for a chemical classification of volcanic rocks based on the total alkali silica (TAS) diagram. Australian Journal of Earths Sciences, 31, 243-255.

Ley 2/2013, de 29 de mayo, de protección y uso sostenible del litoral y de modificación de la Ley 22/1988, de 28 de julio, de Costas. BOE núm. 129.

Ley 4/2017, de 13 de julio, del Suelo y de los Espacios Naturales Protegidos de Canarias.

Mancheri, N., Sundaresan, L., & Chandrashekar, S. (2013). Dominating the World China and the Rare Earth Industry. National Institute of Advanced Studies.

Mangas, J.; Perez Torrado, F.J.; Reguillón, R.M. & Cabrera, M.C. (1992). Prospección radiométrica en rocas alcalinas y carbonatitas de la serie plutónica I de Fuerteventura (Islas Canarias). Resultados preliminares e implicaciones metalogénicas. Actas del III Congreso Geológico de España y VIII Congreso Latinoamericano de Geología. Salamanca. Tomo 3: 389-393.

Mangas, J.; Perez Torrado, F.J.; Reguillón, R.M. & Martin-Izard, A. (1994). Mineralizaciones de tierras raras ligadas a los complejos intrusivos alcalino-carbonatíticos de Fuerteventura (Islas Canarias). Bol. Soc. Esp. Min, 17 (1): 212-213.

Mangas, J.; Perez Torrado, F.J.; Reguillón, R.M. & Martin-Izard, A. 1997. Rare earth minerals in carbonatites of Basal Complex of Fuerteventura (Canary Islands, Spain). En: Mineral Deposit: Research and Exploration, where do they meet? Ed. Mineral deposit Papunen. Balkema, Rotterdan. 475-478.

Mariano A.N. (1989 a). Economic geology of rare Earth minerals. In: Geochemistry and mineralogy of rare Earth elements. Rev. In Mineralogy. Publ. The Mineralogical Society of America, 21, 309-338.

Mariano A.N. (1989 b). Nature of economic mineralization in carbonatites and related rock. In: K. Bell, Carbonatites: genesis and evolution. Ed. Unwin Hyman. London, 149-176.

Menéndez, I., Campeny, M., Quevedo-González, L., Mangas, J., Llovet, X., Tauler, E., …Méndez-Ramos, J. (2019). Distribution of REE-bearing minerals in felsic magmatic rocks and paleosols from Gran Canaria, Spain: Intraplate oceanic islands as a new example of potential, non-conventional sources of rare-earth elements. *Journal of Geochemical Exploration*, *204*(October 2018), 270–288.

Möller, P. (1989). REE (Y), Nb and Ta enrichment in pegamtites and carbonatite-alkalic rock complexes. In: P. Möller, P. Cerny and F. Saupé (eds), Lanthanides, tantalum and niobium, Sp. Pub. Nº 7 SGA. Springuer Verlag, 103-144.

Morteani, Giulio. (1991). The rare earths: their minerals, production and technical use. European Journal of Mineralogy. 3. 641-650.

Muñoz, M., Sagredo, J., de Ignacio, C., Fernández-Suárez, J., & Jeffries, T. E. (2005). New data (U-Pb, K-Ar) on the geochronology of the alkaline-carbonatitic association of Fuerteventura, Canary Islands, Spain. *Lithos*, *85*(1-4 SPEC. ISS.), 140–153.

Ovchinnikova, C.V., Belyatskii, B.V., Valil'eva, I.M., Levskii, L.K., Grachev, A.F., Araña, V, y Mitjavila, J.M. (1995). Sr-Nd-Pb isotope characteritcs of the mantle sources of basalts from Canary Islands. Petrology, 3, 172-182.

Robertson, A. H. F. & Stillman, C.J. (1979b). Submarine volcanic and associated sedimentary rocks of the Fuerteventura Basal Complex, Canary Islands. Geol. Mag., 116: 203-214.

Rollinson, H. R. (1993). Using geochemical data: Evaluation, presentation, interpretation. Pearson-Prestige Hall. Longman group, England. 344 pp.

Schmincke, H. (2004). Volcanism. Springer-Verlag Berlin Heidelberg. X, 234.

Schmincke, H. y Sumita, M. (2010). Geological evolution of the Canary Islands: a young volcanic archipelago adjacent to the old African Continent. Ed. Görres, Koblenz. 200 pp

Schmincke, H.U. (1976). The geology of the Canary Islands. In: Kunkel, G. (Ed.), Biogeography and Ecology in the Canary Islands. Junk, The Hague, 67-184.

Steiner, C., Hobson, A., Favre, P., Stampfli, G.M. & Hernandez, J. (1998). Early Jurassic sea-floor spreading in the central Atlantic, the Jurassic sequence of Fuerteventura (Canary Islands). Geological Society of American Bulletin, 110: 1304-1317.

Sun, S.S. (1980). Lead isotopic study of young volcanic froks from mid-ocean, ocean islands and island arcs. Phli. Trans. R. Soc. London. A297, 409-445.

Sun, W. & McDonough, W. (1989). Chemical and isotopic systematics of oceanic basalts: Implications for mantle composition and processes.

Taylor & McLennan (1985). The continental crust: its composition and evolution. Ed. Blackwell, Oxford, 312 pp.

Thompson, R.N., Morrison M.A., Hendry G.L and parry S.J. (1984). An assessment of the relative roles of a crust and mantle in magma genesis: an elemental approach. Phli. Trans. R. Soc. London, A310, 549-590.

Troll, V.R., Carracedo, J.C., Chapter 8 - The Geology of Fuerteventura, The Geology of the Canary Islands, Elsevier, 2016, Pages 531-582, ISBN 9780128096635

Van Den Bogaard, P. (2013). The origin of the Canary Island Seamount Province-New ages of old seamounts. *Scientific Reports*, *3*(July 2013).

Walker, G.P.L (1990). Geology and volcanology of the Hawaiian Islands. Pacific Sc. 44: 315-347.

Wilson, B.M. (1989). Igneous Petrogenesis A Global Tectonic Approach. Springer Netherlands. Springer Science+Business Media B.V. XX, 466.

Wood, D.A., Joron, J.L. y Treuil, M. (1979). A re-appraisal of the use of trace elements to classify and discriminate between magma series erupted in different tectonic setting. Earth Planet. Sci. Lett. 45, 326-336

Woolley A.R. & Kempe D.R.C. (1989) Carbonatite nomenclature, average, chemical composition and element distribution". En: K. Bell (eds), Carbonatites: genesis and evolution. Ed. Unwin Hyman. London. 1-14.

Woolley, A.R. (1989). The spatial and temporal distribution of carbonatites. In: K. Bell (eds), Carbonatites: genesis and evolution. Ed. Unwin Hyman. London, 15-37

Zazo, C.; Hillarie-Marcel, CL.; Goy, J.L.; Ghaleb, B. & Hoyos, M. (1997). Cambios del nivel del mar-clima en los últimos 250 ka: (Canarias Orientales, España). Bol. Geol. y Minero, 108: 31-41.

7. Attachments

Annex Table 1. Code 4E-research detection limits (in ppm) of every analyzed element reported by different technologies (Data given by www.actlabs.com).

Oxide/Element		4E-research (Detection limit)	Reported by
MAJOR AND MINOR ELEMENTS	Al_2O_3	0.01%	ICP
	CaO	0.01%	ICP
	Fe_2O_3	0.01%	ICP
	K_2O	0.01%	ICP
	MgO	0.01%	ICP
	MnO	0.01%	ICP
	Na_2O	0.01%	ICP
	P_2O_5	0.01%	ICP
	SiO_2	0.01%	ICP
	TiO_2	0.05%	ICP
	LOI	0.01%	ICP
TRACE ELEMENTS	Ag	0.5	ICP/INAA
	As	1	INAA
	Au	1 ppb	INAA
	Ba	1	ICP/INAA
	Be	1	ICP
	Bi	2	ICP
	Br	0.5	INAA
	Cd	0.5	ICP
	Co	0.1	INAA
	Cr	0.5	INAA
	Cs	0.2	INAA
	Cu	1	ICP
	Ga	5 / 1	XRF / ICP-MS
	Ge	0.5	ICP-MS
	Hf	0.2 / 0.1	INAA / ICP-MS
	In	0.1	ICP-MS
	Ir	2 ppb	INAA
	Mo	2	INAA
	Nb	1 / 0.2	XRF / ICP-MS
	Ni	1	ICP
	Pb	5	XRF
	Rb	10 / 2 / 1	INAA / XRF / ICP-MS
	S	0.001%	ICP
	Sb	0.1	INAA
	Sc	0.01	INAA
	Se	0.5	INAA
	Sn	5 / 1	XRF / ICP-MS
	Sr	2	ICP
	Ta	0.3 / 0.01	INAA / ICP-MS
	Th	0.1 / 0.05	INAA / ICP-MS
	Tl	0.05	ICP-MS
	U	0.1 / 0.01	INAA / ICP-MS
	V	5	ICP
	W	1	INAA
	Y	1	ICP
	Zn	2	ICP
	Zr	4 / 1	ICP / ICP-MS

Diego Greca Oteo

TRACE REE	**TRACE LREE**	La	0.05	INAA
		Ce	1 / 0.05	INAA / ICP-MS
		Pr	0.01	ICP-MS
		Nd	1 / 0.05	INAA / ICP-MS
		Sm	0.01	INAA
		Eu	0.05 / 0.005	INAA / ICP-MS
	TRACE HREE	Gd	0.01	ICP-MS
		Tb	0.1 / 0.01	INAA / ICP-MS
		Dy	0.01	ICP-MS
		Ho	0.01	ICP-MS
		Er	0.01	ICP-MS
		Tm	0.005	ICP-MS
		Yb	0.05 / 0.01	INAA / ICP-MS
		Lu	0.01 / 0.002	INAA / ICP-MS
11 + samples			4E-research	€85.50
Add-ons			4E-XRF	€18.00 surcharge
			4E-ICP-MS	€29.75 surcharge

Annex Table 2. Geochemical concentration of every collected sample: oxides in %, trace in ppm and Ir and Au in ppb.

Sample	BE 1	BE 2	BE 3-1	BE 3-2	BE 3-3	BE 3-5	BE 3-6	BE 3-11	BE 5-1	BE 6-1	BE 6-2	BE 7	BE 8-1	BE 8-3	BE 8-4	BE 8-6	BE 8-7	BE 8-8	BE 10
SiO_2	52.26	41.5	47.46	37.88	41.16	40.43	49.84	36.12	5.32	41.32	55.65	41.64	36.51	54.92	11	53.72	38.17	39.25	50.3
TiO_2	2.38	3.78	0.5	3.83	4.69	5.64	0.92	0.29	0.16	4.49	1.07	4.5	3.16	0.37	0.58	0.4	4.1	0.37	2.25
Al_2O_3	13.91	14.8	13.85	10.59	12.4	11.58	20.2	11.02	0.82	13.52	12.94	13.78	12.68	18.96	3.44	19.72	13.83	14.74	13.8
$Fe_2O_3(T)$	14.66	11.3	6.55	13.1	15.17	15.32	5.27	4.38	1.59	15.2	11.83	14.48	11.23	3.41	12.12	4.7	9.06	5.32	12.2
MnO	0.12	0.26	0.08	0.24	0.21	0.19	0.13	0.1	0.04	0.2	0.16	0.17	0.27	0.08	0.27	0.13	0.19	0.32	0.16
MgO	0.63	3.31	3.23	5.42	6.63	7.71	1.12	5.68	4.12	4.93	0.53	7.29	6.1	0.87	1.3	0.43	5.09	1.21	7.23
CaO	3.32	11.1	13.35	15.58	12.08	14.94	4.68	16.31	48.08	10.22	2.51	14.43	17.16	3.61	39.72	3.15	17.21	19.7	10.5
Na_2O	3.39	5.35	0.67	4.47	3.36	2.57	8.49	3.55	0.21	3.75	2.96	2.41	4	6.37	0.41	7.51	4.33	4.42	2.63
K_2O	7.02	2.58	7.86	1.02	1.14	1.02	5.1	3.34	0.16	2.02	7.4	0.98	0.58	6.22	0.3	6.94	0.78	2.06	0.56
P_2O_5	0.36	0.88	0.64	1.48	0.76	0.5	0.18	2.58	0.08	0.72	0.2	0.4	0.64	0.16	2.48	0.18	0.98	0.64	0.22
LOI	2.66	5.21	5.66	6.83	2.32	1.03	3.54	16.55	40.16	2.62	2.62	0.84	8.36	5.14	26.53	2.92	7.06	11.93	0.51
Total	100.7	100	99.85	100.4	99.91	101	99.48	99.93	100.7	99	97.89	100.9	100.7	100.1	98.15	99.79	100.8	99.97	100
FeO	1.22	4.63	1.89	4.76	6.8	8.94	3.1	0.23	0.41	6.16	0.82	8.24	4.69	1.54	1.72	2.03	4.24	2.84	9.28
CO_2	1.57	1.14	2.69	2.89	0.14	0.05	0.25	9.94	35.86	0.41	1.74	0.12	2.57	1.5	22.72	0.13	1.89	6.61	0.08
H_2O+	0.3	2.6	1.3	2.65	2.05	1.15	2.55	1	0.85	2.25	0.25	1.05	3.45	2.8	1.1	2.7	3.15	3.4	0.85
La	53.9	114	468	61.1	57.8	44.1	24.4	270	3.3	77.3	38.9	33.8	51.8	13.6	379	30.1	43.3	143	9.1
Ce	90	190	705	103	105	85	59	430	7	136	55	66	115	26	579	45	84	251	21
Nd	38	78	212	40	57	46	26	130	3	57	14	34	75	11	210	13	40	92	13
Sm	6.7	12	23	7.9	10	10	4.5	17	0.54	11	2.3	7.7	22	1.9	30	2.2	7.9	14	3.7
Eu	2.4	3.95	6.03	2.7	3.28	3.2	1.4	4.68	0.18	3.47	1.35	2.52	8.56	0.49	8.33	0.7	2.9	4.6	1.44
Tb	1	1.5	2.3	1.3	1.2	1.2	0.5	1.9	0.1	1.2	0.7	1	5.1	0.3	3.3	0.3	1.2	1.9	0.7
Yb	1.45	2.47	5.2	1.8	1.52	1.56	1	3.73	0.13	1.84	5.54	1.33	13.5	0.74	6	0.82	2.02	4.23	1.59
Lu	0.19	0.4	0.81	0.26	0.24	0.23	0.16	0.57	0.02	0.27	0.88	0.2	1.89	0.13	1.01	0.13	0.25	0.61	0.23
Ba	1789	825	2973	280	1229	425	3788	1364	35	682	780	345	185	6334	381	2063	249	3253	155
Co	11	24	29	30	45	52	4.4	14	19	49	4.7	54	14	2.5	15	2	12	3.7	43
Cr	7	3	2.2	3	120	72	3.1	2	170	4.2	4.2	130	< 0.5	2.7	1.9	2.2	3.2	0.8	260
Cs	0.4	0.8	0.5	0.6	0.5	< 0.2	0.8	0.2	< 0.2	0.8	< 0.2	< 0.2	0.2	0.5	< 0.2	0.7	0.3	0.4	< 0.2
Cu	106	75	95	120	144	99	13	65	12	95	72	83	9	33	85	1	15	14	116
Ga	38	28	87	8	26	25	32	60	-2	26	96	21	11	21	19	45	7	19	17

Diego Greca Oteo

Hf	8	11	15	15	8.6	8.9	9.5	20	0.4	8	51	6.8	24	8.8	9.1	7.9	17	9.7	3
Nb	166	159	147	117	70	61	157	296	6	95	796	42	120	81	83	87	121	76	16
Ni	traz	9	8	5	93	141	9	9	204	52	7	207	3	4	3	6	6	8	219
Pb	51	16	9	6	7	8	9	23	8	9	82	7	< 5	< 5	10	11	< 5	9	< 5
Rb	95	70	164	33	40	27	81	81	13	55	192	24	21	111	20	101	21	48	18
S	247	3298	744	575	3067	1285	4610	1289	1723	1356	757	285	400	195	1551	5321	854	737	224
Sb	1.6	0.2	0.3	< 0.1	0.1	0.1	0.2	0.2	< 0.1	0.2	0.5	0.1	0.2	< 0.1	0.2	0.1	< 0.1	0.2	< 0.1
Sc	1.8	7.9	1.6	6.3	23	33	1.2	0.7	2	12	2.2	34	6.9	0.6	0.4	0.3	5.1	0.6	23
Sr	397	2745	4860	1284	860	792	1132	3019	718	1022	430	835	1480	1107	5676	949	2208	2949	332
Ta	4.6	7.7	1	3.1	4.3	3.1	2.8	1.3	< 0.3	5	4.6	3	3.9	1.1	1.2	1.3	4.8	0.8	1
Th	4.3	8.4	5	3.6	4.3	3.4	1	18	0.3	6.2	19	2.6	6.8	1.6	5.5	3.6	1.8	9.5	0.9
U	3.6	1.8	3.8	1.2	1.2	0.9	< 0.1	12	0.6	2	55	0.9	2.4	0.4	< 0.5	1.2	0.2	1	0.3
V	208	346	263	328	385	528	212	145	13	362	244	586	322	159	436	159	257	253	225
Y	28	36	66	30	30	28	10	48	< 2	32	36	22	134	8	82	8	32	44	24
Zn	233	129	78	137	164	138	72	136	27	138	208	126	128	71	135	109	91	88	119
Zr	436	436	500	509	363	321	438	77	20	336	5106	223	450	542	170	453	619	613	129
Ag	0.6	< 0.3	< 0.3	< 0.3	< 0.3	1.1	< 0.3	0.4	< 0.3	< 0.3	0.3	0.3	< 0.3	0.4	0.4	< 0.3	0.8	< 0.3	0.4
As	< 1	1	3	< 1	< 1	< 1	< 1	2	< 1	1	2	< 1	< 1	1	3	< 1	< 1	< 1	< 1
Be	4	4	2	3	< 2	< 2	4	4	< 2	< 2	6	< 2	5	2	< 2	4	3	7	< 2
Bi	< 5	< 5	< 5	< 5	10	< 5	< 5	< 5	< 5	< 5	< 5	< 5	< 5	< 5	8	< 5	< 5	< 5	< 5
Br	< 0.5	< 0.5	< 0.5	< 0.5	< 0.5	< 0.5	< 0.5	< 0.5	4.1	< 0.5	< 0.5	< 0.5	< 0.5	0.6	< 0.5	< 0.5	< 0.5	< 0.5	< 0.5
Cd	< 0.5	< 0.5	< 0.5	< 0.5	< 0.5	0.6	< 0.5	1.1	< 0.5	< 0.5	< 0.5	< 0.5	< 0.5	< 0.5	< 0.5	< 0.5	< 0.5	< 0.5	< 0.5
Hg	< 1	< 1	< 1	< 1	< 1	< 1	< 1	< 1	< 1	< 1	< 1	< 1	< 1	< 1	< 1	< 1	< 1	< 1	< 1
Mo	20	4	2	< 2	< 2	< 2	< 2	3	< 2	< 2	< 2	< 2	< 2	< 2	< 2	3	< 2	3	< 2
Se	< 0.5	< 0.6	0.9	< 0.5	< 0.5	< 0.5	< 0.5	1.7	< 0.5	< 0.5	< 0.5	< 0.5	0.8	< 0.5	< 0.5	< 0.5	< 0.5	< 0.5	< 0.5
Sn	< 5	< 5	< 5	< 5	< 5	< 5	< 5	< 5	< 5	< 5	< 5	< 5	< 5	< 5	7	< 5	< 5	< 5	< 5
W	7	< 1	5	< 1	< 1	< 1	< 1	< 1	< 1	< 1	4	< 1	< 1	< 1	18	< 1	1	< 1	< 1
Au	46	4	3	< 2	< 2	< 2	2	< 2	3	< 2	3	< 2	< 2	< 2	< 2	< 2	< 2	< 2	< 2
Ir	< 1	< 1	< 1	< 1	< 1	< 1	< 1	< 1	< 1	< 1	< 1	< 1	< 1	< 1	< 1	< 1	< 1	< 1	< 1

BE 10-3	BE 11-1	BE 11-5	BE 12	BE 13	BE 15	BE 16-1	BE 16-2	BE 16-3	BE 18-1	BE 18-2	C 1	C 2	P 28	P 30	P 31	P 33	P 36	P 38	P 43
35	45.92	56.78	34.3	46.6	55.3	27.04	51.45	55.07	55.26	47.75	41.75	41.94	1.9	51.18	51.2	62.2	28.1	33.7	60.2
6.2	1.53	1.22	8.29	2.29	0.79	1.53	0.27	0.79	0.38	2.4	3.53	3.4	0.04	1.18	0.89	0.24	4.98	4.82	0.24
9.88	16.59	13.85	8.61	14.2	14.4	9.58	14.62	17.99	16.86	16.26	10.72	10.33	0.67	18.15	18.2	19.5	8.16	11.6	18
14.42	8.55	9.09	16.4	11	9.85	10.47	7.64	5.77	4.36	8.18	13.02	12.63	1.41	7.39	5.8	3.81	17.7	16.2	3.61
0.26	0.31	0.16	0.26	0.46	0.17	1.45	0.38	0.21	0.14	0.19	0.18	0.17	0.93	0.17	0.16	0.11	0.25	1.1	0.16
6.68	1.45	1.15	6.65	2.35	0.81	4.92	0.7	1.27	1.69	3.18	14.73	15.19	0.4	1.33	1.37	0.63	10.2	2.84	0.84
17.42	10.68	4.46	17	9.83	3.58	28.42	7.18	4.29	2.68	8.12	11.68	11.79	50.6	4.12	5.81	1.71	13.4	9.47	2.74
2.1	4.5	7.8	2.26	4.93	4.29	0.69	1.42	2.94	2.56	4.17	2.84	2.86	0.32	5.56	7.77	9.87	1.8	3.85	6.39
1.34	3.36	0.64	0.94	3.76	6.12	1.74	9.9	7.92	9.04	4.96	1.1	0.96	0.08	5.58	2.72	0.76	2.5	1.48	5.34
1.52	0.34	0.7	1.9	0.36	0.12	1.02	0.26	0.3	0.06	0.46	0.68	0.64	0.26	0.24	0.32	0.08	2.06	3.4	0.08
4.87	7.64	4.53	3.15	3.07	3.21	7.81	5.56	4.06	5.16	4.82	< 0,01	< 0,01	40	4.82	5.68	0.79	8.6	3.27	2.42
99.69	100.87	100.38	99.7	98.9	98.6	94.67	99.38	100.6	98.18	100.49	100.1	99.81	96.6	99.71	99.9	99.6	97.7	91.7	100
6.17	1.59	0.34	5.71	3.09	0.95	1.13	1.22	1.13	0.77	4.83	8.22	8.9	0.73	2.33	2.83	1.16	4.9	2.38	0.77
2.62	3.96	2.75	0.97	0.76	2.05	4.38	3.36	1.9	1.83	1.67	0.01	0.01	34.5	1.17	2.42	0.01	4.63	0.04	1.04
1.25	0.65	0.9	1.75	1.85	0.35	0.65	0.5	0.35	0.7	0.45	0.35	0.25	0.4	2.8	1.3	0.35	1.45	1.4	0.4
154	62	81.4	311	236	34.3	1900	297	177	62.4	78.5	42.7	39	734	56.7	67.6	257	101	270	342
279	78	113	352	427	47	2300	517	265	97	123	87	77	1140	132	121	344	190	550	443
125	22	40	114	165	15	650	184	76	25	45	44	40	440	62	45	74	83	580	103
22	4.7	8.7	26	27	2.4	73	22	9.6	3.5	7.1	8.3	7.8	65	10	6.8	7.3	21	420	13
6.93	1.79	3.49	9.86	8.78	1.03	27.7	6.93	3.06	1.13	2.3	2.45	2.4	20.3	3.47	2.21	1.98	9.8	260	3.81
2.7	1.1	1.9	4.5	3.8	0.4	8.9	2.4	1.3	0.6	0.8	1	0.9	8.8	1.2	0.8	0.6	9	130	1.6
3.12	3.63	2.86	4.97	9.99	2.64	12.9	10	3.16	2.09	1.89	1.37	1.29	18.5	2.97	1.86	1.94	19.4	69.3	3.89
0.41	0.56	0.41	0.63	1.5	0.48	1.85	1.61	0.52	0.32	0.28	0.18	0.18	2.85	0.45	0.3	0.31	2.77	10.3	0.66
260	2590	240	226	3622	742	5400	7903	2217	683	905	644	589	6800	4373	6281	2039	968	####	1600
44	8.5	9.8	64	12	4.8	12	11	5.5	4.9	17	65	64	2.8	4.2	5.2	3.7	57	20	3.7
0.5	1.6	4.2	0.5	4.2	4.3	15	3.1	2.2	4.2	30	780	1100	4	2.8	3.3	3.2	12	37	2.7
0.4	0.3	< 0.2	0.6	0.7	0.3	< 0.2	< 0.2	0.5	0.3	1.2	0.5	0.3	< 0.2	0.7	0.9	< 0.2	4.2	< 0.2	0.5
222	27	136	268	16	59	31	33	28	7	41	54	84	13	15	21	19	96	108	15
8	49	78	10	33	63	51	60	54	47	34	15	15	-2	53	59	33	24	18	41
8.5	14	11	10	20	27	8.9	110	18	11	9.2	5.1	4.8	< 0.2	39	16	24	9.4	4.5	28

Diego Greca Oteo

200	139	117	463	392	107	605	455	238	141	117	66	62	18	399	249	269	241	2163	383
14	5	8	27	9	10	21	10	12	13	43	441	492	7	7	8	11	60	44	8
5	43	18	11	< 5	14	325	252	39	25	14	8	< 5	82	8	6	11	87	1545	48
34	74	15	25	77	169	62	158	189	227	111	36	37	24	113	99	21	135	45	175
318	1566	673	2674	2287	508	5269	278	1965	2152	4247	< 50	464	7175	4034	1446	2554	5050	####	3950
0.3	0.2	0.7	0.3	0.3	0.3	1.3	0.7	0.3	0.4	0.3	0.2	< 0.1	0.5	0.3	0.2	0.3	3	5.5	0.5
12	1.4	5.7	14	3.9	1.2	3.6	1.4	1.1	0.4	11	30	28	2.4	1	0.5	0.3	52	10	0.4
1829	5570	544	1506	4146	743	5000	1914	1670	372	1676	900	798	< 1	1907	4840	2137	801	3750	1960
11	1.9	1.6	17	9	1.3	3.6	3.3	2.6	1.5	2.9	3.6	3.3	0.6	10	5	3.5	2.9	5.5	6.4
13	2.7	45	5.2	21	4.6	95	65	48	25	11	3.5	3.3	20	10	5.3	43	90	1100	70
2.5	2.7	6	7.3	5.5	6.9	34	87	6.3	3.1	3.7	0.7	0.8	10	6.2	13	13	2.1	7.8	14
434	305	166	372	421	178	445	92	170	126	256	295	279	6	221	108	76	516	511	45
52	48	66	78	104	20	252	88	38	20	26	24	18	234	30	24	24	296	500	76
133	208	130	147	297	158	711	387	177	163	159	126	94	374	118	234	102	227	603	176
286	909	692	373	1137	1992	490	6949	1118	579	558	231	222	75	2902	1217	1458	363	760	1270
0.5	0.3	0.5	0.5	0.4	< 0.3	5.6	0.8	0.8	< 0.3	0.7	< 0.3	< 0.3	1.3	0.5	0.9	0.7	0.9	3.5	0.6
< 1	1	8	< 1	3	< 1	16	10	2	2	2	< 1	< 1	< 1	2	1	2	39	52	3
< 2	10	10	< 2	4	5	40	2	13	4	5	< 2	< 2	< 2	4	2	3	15	7	4
< 5	< 5	< 5	< 5	< 5	< 5	< 5	< 5	< 5	< 5	< 5	< 5	< 5	< 5	< 5	< 5	< 5	< 5	< 5	< 5
< 0.5	< 0.5	< 0.5	< 0.5	5.2	< 0.5	< 0.7	< 0.5	< 0.5	7.4	1.5	< 0.5	< 0.5	< 0.5	3.9	1.4	10	16	< 0.7	6.5
< 0.5	0.7	< 0.5	< 0.5	< 0.5	< 0.5	1.2	0.7	< 0.5	< 0.5	0.5	< 0.5	< 0.5	2.1	< 0.5	< 0.5	< 0.5	0.6	< 0.5	< 0.5
< 1	< 1	< 1	< 1	< 1	< 1	< 1	< 1	< 1	< 1	< 1	< 1	< 1	< 1	< 1	< 1	< 1	< 1	< 1	< 1
5	4	11	9	< 2	5	2	36	7	< 1	3	< 2	< 2	< 2	3	< 2	6	80	540	8
< 0.5	0.5	< 0.5	< 0.5	< 0.5	< 0.5	0.8	< 0.7	< 0.5	< 0.5	< 0.5	< 0.5	< 0.5	< 0.5	< 0.5	< 0.5	< 0.5	< 0.5	< 1.8	< 0.5
< 5	7	< 5	< 5	< 5	< 5	< 5	< 5	7	< 5	< 5	6	< 5	< 5	< 5	< 5	< 5	12	28	8
5	< 1	4	< 1	< 1	3	< 3	7	< 1	< 1	< 1	< 1	< 1	< 1	< 1	< 1	< 1	13	48	< 1
< 2	< 2	5	< 2	< 2	2	6	< 2	< 2	< 2	< 2	< 2	< 2	< 2	< 2	< 2	54	< 2	< 2	< 2
< 1	< 1	< 1	< 1	< 1	< 1	< 1	< 1	< 1	< 1	< 1	< 1	< 1	< 1	< 1	< 1	< 1	< 1	< 1	< 1

Diego Greca Oteo

P 45	P 46	P 46-1	P 48	P 49	P 51	P 52	PA 1	PA 2	PA 4	PA 5	PA 6	PA 7-2	PA 7-3	PA 8-1	PA 8-2	PA 8-3	PA 8-4	PA 11	PA 12
61.6	57.3	13.31	56.54	49.8	41.7	58.5	41	42.3	53.88	55.1	11.8	48.4	12.5	11.4	4.11	18.47	5.21	39.49	8.26
0.22	0.24	0.45	0.53	0.39	4.7	0.77	5.43	4.45	1.04	0.21	0.05	0.84	0.11	0.16	0.16	0.14	0.59	2.34	0.42
19.3	18.4	4.55	19.36	30.62	14.3	17	13.1	14.2	18.87	19.79	3.66	19.7	5.09	1.49	1.33	6.57	1.59	14.53	1.81
2.71	4.09	10.02	4.42	1.18	14.1	4.35	13.7	12.3	4.88	2.91	0.94	5.6	2.03	3.81	1.01	2.43	4.39	10.86	7.29
0.1	0.14	0.47	0.45	0.03	0.23	0.31	0.34	0.26	0.18	0.22	0.27	0.28	0.28	0.33	0.25	0.2	0.23	0.35	0.27
1.1	0.45	0.31	0.99	0.26	5.53	1.28	4.84	4.97	1.36	0.18	4.59	1.22	0.76	1.49	0.31	0.24	0.58	4.26	3.24
2.63	4.67	36.78	4.64	1.4	11.4	5.55	13.2	10.4	4.44	2.21	39	7.96	44	42.3	49.35	36.2	48.5	14.21	40.74
9.34	7.59	2.42	9.11	4.94	3.56	8.14	3.8	2.97	5.89	10.72	1.16	8.38	1.65	1.58	0.81	1.63	0.37	6.4	0.96
1.36	3.64	0.4	1.14	6.58	1.3	1.14	2.38	3.64	4.6	4.96	1.4	1.32	1.02	0.18	0.08	2.52	0.14	0.38	0.32
0.12	0.46	1.06	0.36	0.28	1.18	0.56	1.12	1.28	0.26	0.08	0.04	0.34	0.2	3.74	0.52	0.52	5.42	1.9	5.14
2.24	3.84	28.31	2.46	4.29	0.67	2.09	1.44	1.7	3.94	2.28	36.7	5.04	33.1	29.5	39.65	28.84	31.68	5.86	29.23
101	101	98.09	99.99	99.77	98.6	99.7	100	98.4	99.33	98.64	99.6	99.1	101	95.9	97.57	97.76	98.7	100.6	97.68
0.59	1.4	2.83	1.83	0.25	7.05	1.43	6.3	5.24	2.03	0.59	0.17	1.31	0.5	0.86	0.14	1.31	0.95	4	2.38
0.56	1.52	25.22	0.12	0.12	0.02	0.86	0.03	0.06	0.52	0.06	29.3	0.44	28.4	25.5	33.84	25.24	26.74	0.62	24.7
0.65	0.55	0.5	0.9	0.75	1.05	0.6	1.2	1.05	2.3	1.65	0.2	2.7	0.85	0.2	0.3	0.75	0.15	4.65	0.4
48.1	239	944	200	117	88.6	537	232	144	116	250	59.5	163	440	635	500	430	726	112	232
93	401	1500	384	190	167	858	430	265	182	342	72	292	721	1160	850	755	1200	185	316
34	151	462	159	85	80	290	183	121	58	73	18	112	234	494	318	267	550	76	114
5.2	23	71	28	12	13	40	31	19	7.6	7.4	2.1	15	34	69	46	42	73	12	18
1.8	6.53	19.8	7.86	3.44	4.36	13	9.14	5.74	2.38	1.92	0.66	4.98	9.92	21.4	13.9	12.7	26.3	4.2	6.25
1	2.4	6.6	2.6	1.7	1.6	6.7	3.5	2.3	0.9	1.2	0.8	2	3.7	8.2	4.6	4.3	9	1.8	3.1
4.14	5.55	8.63	4.98	4.47	2.15	14.4	5.41	3.23	2.56	2.06	2.48	2.97	7.72	8.85	7.51	7.28	9.86	3.55	6.68
0.67	0.81	1.19	0.74	0.74	0.28	1.8	0.7	0.42	0.34	0.28	0.36	0.45	1.08	1.25	1	0.99	1.32	0.52	0.9
2690	5073	1800	1882	2900	1110	3217	949	1266	1752	1644	825	3767	1000	503	699	1880	378	164	382
3.1	5.6	4.6	3.3	2.7	37	6	22	29	5.9	2.2	1.2	5	2.2	5.8	1	3	17	23	9.5
3.7	3.1	2.4	0.5	1.7	7.2	6.5	2.6	1.9	2.7	1.1	2.6	2.2	< 0.5	1	< 0.5	< 0.5	< 1.3	1.3	6.4
< 0.2	0.5	< 0.2	0.6	0.5	< 0.2	0.6	0.6	0.7	1.2	2.7	< 0.2	1.5	< 0.2	< 0.2	< 0.2	0.3	< 0.2	0.5	0.5
18	19	11	17	10	25	32	30	40	11	4	9	20	10	10	4	20	74	19	23
101	49	22	57	113	21	40	24	25	39	54	5	25	16	7	-2	17	3	12	14

Diego Greca Oteo

36	52	9.9	24	38	9.1	30	18	15	17	24	7.1	10	15	6.1	2	7.7	3.1	18	6.1
712	776	178	1111	2068	116	523	353	212	185	296	46	287	204	89	104	117	416	310	42
10	8	1	10	5	44	12	11	13	6	3	1	6	13	2	6	2	9	8	17
10	9	18	25	16	< 5	25	11	13	24	41	15	7	16	11	19	15	23	9	14
35	51	28	35	120	30	27	52	84	117	160	40	39	37	24	20	56	19	17	35
2517	896	479	1131	3028	1065	155	8916	5638	3248	12100	898	5819	1091	372	972	725	2142	2910	3929
0.3	0.3	0.3	0.3	0.3	< 0.1	0.4	0.4	0.3	0.3	0.3	0.2	0.3	0.3	0.3	0.2	0.2	0.4	0.3	0.3
1.7	1.6	0.4	1.6	0.7	17	3.4	11	16	2.4	0.3	0.6	2.4	0.4	0.5	0.3	0.3	0.7	2.4	3.7
779	1218	< 1	1062	3304	1752	2214	1923	1350	2102	2902	756	2174	6848	7020	247	7166	6953	2752	7366
9.2	18	5.2	22	37	6.6	21	22	12	6.7	5.1	1.2	4.9	2.7	1.8	3.3	3.7	11	3.7	0.5
49	49	23	52	83	3.3	130	11	11	23	47	24	13	21	46	7.6	12	51	5.1	4.3
100	62	10	48	560	1.9	13	2.1	1.9	6.2	13	2.9	4	9.5	3.4	1.5	19	4.1	1.1	2.4
141	63	156	64	145	340	129	463	363	88	24	16	189	31	79	19	47	45	310	501
36	66	142	70	58	44	198	92	54	30	24	8	48	100	158	120	94	208	64	70
44	70	191	92	27	152	197	209	176	137	240	219	136	60	87	54	48	78	129	138
4158	3866	330	1507	3204	478	1580	835	674	1108	1419	446	664	1470	249	236	455	311	424	345
1.4	1.1	1.7	1.6	1.3	0.7	0.5	0.9	0.5	< 0.3	0.4	0.4	1.1	< 0.3	1.2	1.1	0.7	1.1	< 0.3	0.7
3	2	2	< 1	5	< 1	3	1	2	1	2	3	2	< 1	< 1	< 1	< 1	< 1	3	10
4	3	< 2	5	15	< 2	14	2	< 2	6	10	2	4	6	4	< 2	< 2	< 2	< 2	2
< 5	< 5	< 5	< 5	< 5	< 5	< 5	< 5	< 5	< 5	< 5	< 5	< 5	< 5	6	< 5	< 5	< 5	< 5	< 5
4.5	4.5	< 0.5	4.6	4.2	< 0.5	< 0.5	4.3	< 0.5	5.4	2.8	3.2	5.8	< 0.5	3.2	< 0.5	< 0.5	< 0.5	8	3.4
< 0.5	< 0.5	< 0.5	< 0.5	< 0.5	< 0.5	< 0.5	< 0.5	< 0.5	< 0.5	0.6	1	< 0.5	< 0.5	< 0.5	< 0.5	< 0.5	< 0.5	< 0.5	< 0.5
< 1	< 1	< 1	< 1	< 1	< 1	< 1	< 1	< 1	< 1	< 1	< 1	< 1	< 1	< 1	< 1	< 1	< 1	< 1	< 1
3	< 2	< 2	4	30	< 2	< 2	6	< 2	4	9	2	8	< 2	< 2	< 2	< 2	< 2	< 2	< 2
< 0.5	< 0.5	< 0.5	< 0.7	0.7	< 0.5	< 0.6	< 0.5	< 0.5	< 0.5	< 0.5	< 0.5	< 0.5	< 0.5	< 0.6	< 0.5	< 0.5	< 1.3	1.3	< 0.6
< 5	< 5	< 5	7	< 5	< 5	9	< 5	< 5	< 5	7	< 5	9	< 5	< 5	< 5	< 5	< 5	10	< 5
< 1	< 1	< 1	< 1	< 1	< 1	< 1	< 1	< 1	< 1	< 1	< 1	< 1	< 1	< 1	< 1	< 1	12	< 1	< 1
< 2	< 2	< 2	< 2	< 2	< 2	3	< 2	< 2	< 2	< 2	< 2	< 2	< 2	< 2	< 2	< 2	< 2	< 2	< 2
< 1	< 1	< 1	< 1	< 1	< 1	< 1	< 1	< 1	< 1	< 1	< 1	< 1	< 1	< 1	< 1	< 1	< 1	< 1	< 1

Diego Greca Oteo

PA 13	PA 14	PA 16	PA 18	PA 18-2	PA 18-3	PA 18-6	PA 18-7	S 1	S 2	S 3	S 4	S 5-1	S 5-2	S 6
45.71	57.99	62.8	37.3	44.6	56.23	6.38	51.96	70.05	71.16	63.68	68.12	52.3	4.03	46.35
2.38	0.09	0.26	6.4	4.94	1.32	0.12	1.26	0.2	0.21	0.8	0.15	0.91	0.22	2.38
13.75	22.68	20.3	9.04	15.5	19.83	1.96	15.37	15.75	14.5	17.31	15.55	19.9	1.24	18.64
11.99	1.56	2.84	21	11.4	4.52	31.1	6.47	2.08	1.89	3.88	3.5	4.85	12.31	10.12
0.48	0.06	0.04	0.2	0.14	0.11	0.16	0.21	0.14	0.24	0.27	0.22	0.19	1.21	0.14
2.38	0.38	0.38	8.5	4.15	1.02	2.3	1.36	0.78	0.32	0.58	0.17	1.02	1.15	3.78
9.88	1.01	0.48	13	9.95	2.08	29.8	6.26	0.49	0.24	1.54	0.33	3.9	41.98	13.28
5.09	11.12	10	2.08	4.53	6.18	0.22	4.07	5.53	6.35	7.73	7.43	6.27	0.45	3.06
3.58	1.22	1.3	0.88	2.34	6.06	0.06	6.8	4.84	4.28	4.18	4.38	4.6	0.52	0.66
0.38	0.06	0.08	0.36	1.46	0.26	1.62	0.3	0.06	0.14	0.18	0.14	0.22	0.78	0.3
3.16	3.74	1.73	0.62	1.93	2.71	24.8	3.5	0.78	1.02	0.43	0.29	3.86	34.05	0.72
98.77	99.92	100	99.4	101	100.3	98.4	97.55	100.7	100.35	100.57	100.3	98	97.93	99.43
3.01	1.49	1.76	7.68	5.32	1.93	0.48	1.86	0.48	< 0,01	1.93	1.74	2.4	0.81	5.44
0.87	0.11	0.05	0.01	0.14	0.2	16.1	0.69	0.01	0.03	0.05	0.02	0.48	27.14	0.71
1.8	3.05	1.3	0.8	1.7	2.15	3.5	1.9	0.65	0.6	0.2	0.7	0.7	1.4	0.3
217	111	18.5	40	87.7	119	719	132	70	17.2	103	114	127	2700	18.4
418	131	28	84	150	186	830	228	112	42	174	192	196	3500	37
165	24	9	46	72	61	195	73	31	20	59	58	57	1000	20
24	2.2	1.3	8.7	13	9.2	20	9.7	4.4	4.7	9	9.4	7.8	110	4.4
8.09	0.56	0.5	2.7	4.11	2.55	5.46	2.79	1.15	1.1	3.39	1.82	2.5	30.7	1.77
3.8	0.1	0.2	1.2	1.4	1.2	1.7	1	0.6	1	1.2	1.3	0.9	12	0.6
9.89	0.41	1.87	1.43	1.7	2.28	3.26	1.63	1.8	3.25	3.71	3.85	2.6	16.7	1.14
1.32	0.07	0.28	0.21	0.23	0.31	0.52	0.26	0.3	0.45	0.56	0.53	0.42	2.61	0.17
4020	540	1318	309	684	1158	211	12318	519	258	1622	501	2699	2526	215
13	1	4.3	59	37	4.9	140	7.8	1	0.8	0.6	0.5	5.3	20	25
1.8	3.8	5.7	6.2	0.7	1.9	0.6	2.3	3.4	3.1	4.6	4.3	5	7	43
0.9	0.5	0.3	< 0.2	0.6	1	< 0.2	0.5	2.2	0.4	0.6	0.8	0.8	1.1	< 0.2
18	10	22	111	196	28	1021	66	2	4	6	8	6	122	68
29	40	45	23	26	32	2	41	31	32	32	35	43	3	21
20	6.7	21	8.7	8.2	11	2.7	8.6	11	15	18	22	9.7	1.5	3.5

Diego Greca Oteo

421	72	62	61	99	183	44	372	123	226	172	258	165	470	25
12	2	7	117	51	5	74	7	7	5	5	9	3	20	64
10	21	6	11	13	16	30	7	13	20	15	17	9	81	6
77	21	28	25	51	134	11	162	205	138	99	126	111	48	24
961	1596	1852	5199	2302	4582	7868	5622	< 50	1314	278	782	1642	3867	947
0.3	0.2	0.2	0.2	0.3	0.6	1.3	0.3	0.5	0.7	0.4	0.3	0.2	1.3	0.1
3.9	0.1	0.3	37	11	1.1	0.2	2	0.6	2.9	0.8	2	1.7	0.8	18
4060	2478	1007	591	1808	1376	2412	2792	115	32	255	20	3573	< 1	1282
9.8	0.8	0.9	3.1	4.2	8.9	0.3	5.6	6.3	12	7.3	12	3.7	1.8	1.5
19	16	3.8	3.3	9.9	19	27	8	34	25	14	23	12	25	1.7
4.6	5.4	6.6	1	3.3	5.9	8.9	1.5	10	5.3	3.6	2.7	2.4	< 0.6	0.6
451	14	98	666	282	68	128	252	15	8	12	2	113	135	249
120	4	8	28	34	32	44	26	18	36	40	40	30	286	20
236	70	49	191	94	85	189	196	77	147	164	233	140	2424	103
1085	640	1534	347	427	685	255	494	360	423	958	872	591	163	120
0.7	< 0.3	0.5	1	1.4	< 0.3	0.9	< 0.3	< 0.3	< 0.3	< 0.3	0.4	< 0.3	6.6	0.8
3	2	2	< 1	< 1	2	40	4	2	2	2	< 1	2	41	< 1
3	4	3	< 2	< 2	3	6	3	6	6	5	9	4	< 2	< 2
< 5	< 5	7	< 5	< 5	< 5	< 5	< 5	< 5	8	7	< 5	< 5	< 5	9
< 0.5	3.1	3.2	2.3	3.1	3.3	11	5	< 0.5	22	2.2	< 0.5	2.2	12	< 0.5
< 0.5	< 0.5	< 0.5	0.7	< 0.5	< 0.5	4.8	< 0.5	< 0.5	< 0.5	< 0.5	< 0.5	< 0.5	8.2	0.5
< 1	< 1	< 1	< 1	< 1	< 1	< 1	< 1	< 1	< 1	< 1	< 1	< 1	< 1	< 1
< 2	4	5	5	< 2	7	11	< 2	7	5	4	3	< 2	< 2	< 2
< 0.6	< 0.5	0.9	< 0.5	< 0.5	< 0.5	< 0.5	< 0.5	< 0.5	< 0.5	< 0.5	< 0.5	< 0.5	< 0.9	< 0.5
8	6	< 5	< 5	< 5	< 5	< 5	< 5	7	9	< 5	10	< 5	< 5	< 5
< 1	< 1	< 1	< 1	< 1	< 1	< 1	< 1	3	3	< 1	< 1	< 1	< 3	< 1
< 2	2	3	6	10	< 2	6	< 2	< 2	< 2	< 2	< 2	< 2	8	< 2
< 1	< 1	< 1	< 1	< 1	< 1	< 1	< 1	< 1	< 1	< 1	< 1	< 1	< 2	< 1